Fakultät für Umwelt und Natürliche Ressourcen

Professur für Hydrologie

der Albert-Ludwigs-Universität Freiburg i. Br.

Christoph Ries

Streamflow drought characteristics in Australia

Referentin: Prof. Dr. Kerstin Stahl

Koreferent: apl. Prof. Dr. Jens Lange

Master thesis (MSc Environmental Sciences)

Freiburg im Breisgau, Mai 2017

Content

List of Figures

List of Maps

List of Tables

List of Annex

Keywords

Hydrological drought

Meteorological drought

Streamflow

Australia

SPEI

SPI

Abstract

Many drought impacts on the Australian continent are related to streamflow anomalies and dry river beds. However, the national drought monitoring and early warnings system is mainly based on meteorological drought indicators that may or may not directly be linked to hydrological drought signals. To bridge this gap, this thesis evaluates to what extent meteorological drought indicators can be used to predict streamflow patterns and streamflow anomalies in Australia. Long term streamflow data for 152 hydrological reference stations was combined with monthly precipitation and temperature data from 1973 to 2014 to receive three indicator types: the 1 month standardized streamflow index (SSI), the 1 to 24 month Standardized Precipitation Index (SPI) and the 1 to 24 month Standardized Precipitation and Evapotranspiration Index (SPEI).

In part I of the thesis, the correlation between the SSI and the different accumulation periods of SPI/SPEI was analyzed for all 152 stations, grouped into seven regional clusters. In part II, the likelihood of low flow occurrence was assessed as a function of SPEI for selected stations in southeast Australia using logistic regression. Additionally, the modelled likelihood time series were checked for significant trends over time.

The results revealed a continental trend from southeast to northwest visible in the maximum correlation strength, the accumulation period at which the highest correlations are reached and the choice of the indicator. This trend coincided with the general shift in annual precipitation on the continent with the southeast becoming drier (high maximum correlations, short response times, pronounced superiority of SPEI) and the northwest becoming wetter (lower maximum correlations, longer response times, slight superiority of SPI). The results in part II showed that SPEI has a high potential to be used as predictor for low flow occurrence. Seasonal goodness of fit (area under the ROC curve) was lowest in autumn, possibly due to a general change of the autumn climate in the region.

The results strengthen the assumption that increased temperature have a strong impact on the Australia hydrosphere. The results from the logistic regression analysis may provide valuable information for regional stakeholders when planning and managing future drought scenarios and assessing ecological and hydrological risks in the region.

Zusammenfassung

Niedrige Flusspegel haben in Australien in jüngster Vergangenheit große Dürreschäden verursacht und die Dürresituation in vielen Teilen des Landes verschärft. Das australische Dürre-Frühwarnsystem basierte bislang hauptsächlich auf der Analyse meteorologischer Zeitreihen, vornehmlich von Niederschlagsdaten. Diese spiegeln jedoch die hydrologische Situation nur bedingt wider. Diese Arbeit hat zum Ziel, die Aussagekraft von meteorologischen Indikatoren (SPI, SPEI) in Bezug auf hydrologische Signale und hydrologische Extremereignisse zu testen. Grundlage bildet ein Langzeit-Datensatz bestehend monatlichen Abfluss-, Temperatur und Niederschlags-werten von 152 hydrologischen Messstationen für den Zeitraum 1973 bis 2014.

Im ersten Teil der Arbeit wurden die Korrelationsstärke von SSI und SPI/SPEI und Reaktionszeit der Fließgewässer auf unterschiedliche Zeitskalen von SPI und SPEI untersucht. Die Ergebnisse zeigen, dass die Korrelation im gemäßigten Südosten des Kontinents am stärksten war und in Richtung des tropisch geprägten Nordwestens abnahm. Gleichzeitig nahm die Reaktionszeit in dieselbe Richtung zu. Dieser Trend stimmt überein mit einer Verlagerung der kontinentalen Niederschläge in Richtung Nordwesten im selben Zeitraum und bestätigt Schlussfolgerungen anderer Studien, nach denen sich erhöhte Temperatur- und Evapotranspirationswerte negativ auf die Fließgewässer im australischen Südosten auswirken.

Im zweiten Teil der Arbeit wurde mittels logistischer Regression die Wahrscheinlichkeit für das Auftreten von Niedrigwasser (definierter Grenzwert: monatliches 10%-Perzentil) in abhängig von SPEI modelliert. Anschließend wurde mittels linearer Regression geprüft, an welchen Stationen das Niedrigwasserrisiko signifikant gestiegen ist. Die Ergebnisse zeigen, dass ein jahreszeitlich spezifischer SPEI ein hohes Vorhersagepotential für Niedrigwasserereignisse in der Region besitzt. Eine hohe Zahl von Messstationen zeigte einen signifikanten Anstieg des Niedrigwasserrisikos in der Region um Melbourne. Jahreszeitliche Unsicherheiten waren am stärksten im Herbst – möglicherweise als Folge eines generellen Wandels des regionalen Herbstklimas in den vergangenen Jahrzehnten.

Die Ergebnisse der logistischen Regression haben das Potential, die Entscheidungsgrundlage regionaler Interessensgruppen beim Planen und Bewältigen künftiger Dürreereignisse zu verbessern.

1 Introduction

Droughts pose a growing risk to water security and water availability in many regions of the world (Collins et al., 2016; Hannaford et al., 2011; WMO, 2006). In Australia, the recent "Millennium drought", one of the worst droughts on record for the continent, has raised intensified attention to the issue (Kiem et al., 2016; van Dijk et al., 2013; Cai et al., 2009; Cai and Cowan, 2008b; Economist, 2007).

At present, Australian drought monitoring and early-warning systems are mainly based on meteorological drought indicators (Deo et al., 2016; Mpelasoka et al., 2008; WMO, 2006). Meteorological indicators have gained growing popularity in drought research as they require limited data input, i.e. precipitation and temperature, and can thus be easily calculated for different climate zones and land types including remote areas that would be otherwise difficult to monitor (Barker et al., 2016; van Lanen et al., 2016; Haslinger et al., 2014; Vicente-Serrano et al., 2012a).

However, a wide range of drought impacts are not related to recent weather events but to hydrological anomalies, i.e. low streamflows (van Lanen et al., 2016; Vicente-Serrano et al., 2014; Hannaford et al., 2011). The relationship between meteorological and hydrological anomalies is often not evident (Hannaford et al., 2011; WMO, 2006). For example, a short-term shortage in precipitation does not automatically lead to dry river beds if the input deficit is compensated by groundwater inflow and full catchment storages. Also, there can be a noticeable delay between the cessation of rainfall and the moment at which this deficit becomes visible in declining water levels in rivers (van Lanen et al., 2016; WMO, 2006).

Streamflow data is often sparse and incoherent, especially in Australia where rivers pass through hardly accessible territories. Therefore, knowing if and to what extent meteorological drought indicators can be used to predict streamflow anomalies may help to improve drought monitoring and early warning products for Australia. The purpose of this study is to explore this relationship in greater detail. The key research questions are:

1. Are meteorological drought indicators related to streamflow anomalies in Australia?
2. Are meteorological drought indicators related to the occurrence of low flow in southeast Australia?
3. Did the risk of low flow increase in the greater Melbourne area between 1974 and 2014?

1.1 A short history of drought in Australia

Since the beginning of instrumental weather records droughts have been a regularly occurring feature of the hydro-meteorological climate in Australia (Kiem et al., 2016; Dai, 2011; WMO, 2006). Droughts have hit virtually every region of the continent regardless of climate zones, temperature or rainfall regimes (Verdon-Kidd and Kiem, 2009).

Over the last century, Australia witnessed three major droughts (Kiem et al., 2016; CSIRO, 2015). The earliest on record, the "Federation drought" (1885 – 1903), hit the eastern part after low rainfalls in spring and summer. The second, the "World War II drought" (1937 – 1945), was the only major drought affecting the northwest and the southeast simultaneously. And third, the recent "Millennium drought" (2000 – 2010) is considered the most severe one and had strong impacts on the agricultural industry in southeast by partly causing irrigation stops in the Murray-Darling River Basin (CSIRO, 2015; Verdon-Kidd and Kiem, 2009; Economist, 2007). Additionally, many less severe drought events were recorded. The "El Niño drought" (1982 – 1983) (Deo et al., 2016; Stone, 2014) resulted from anomalies in the Southern Oscillation and was known for bringing large sand storms to the city center of Melbourne.

Although droughts can be simply defined as "a lack of water" (van Loon et al., 2016) every major and minor drought event in Australia have had its unique fingerprint and varied significantly in their severity, duration, spatial extent and causative mechanisms (Kiem et al., 2016; Verdon-Kidd and Kiem, 2009).

Recent studies suggest that the Millennium drought differed distinctly from other droughts on the continent (van Dijk et al., 2013; Yu et al., 2010; Nicholls, 2004). Additionally to low rainfall intensities this major drought event was accompanied by a long lasting heat wave that spread over southern and eastern Australia and prompted high evapotranspiration rates (van Dijk et al., 2013). This exacerbated the drought situation in many regions. Similar effects of high temperatures on the severity of a drought were also observed during the severe 2003 drought in Europe (Teuling et al., 2013). This evoked the theory that nature of droughts might be about to change worldwide (Nicholls, 2004).

1.2 Climate drivers related to droughts in Australia

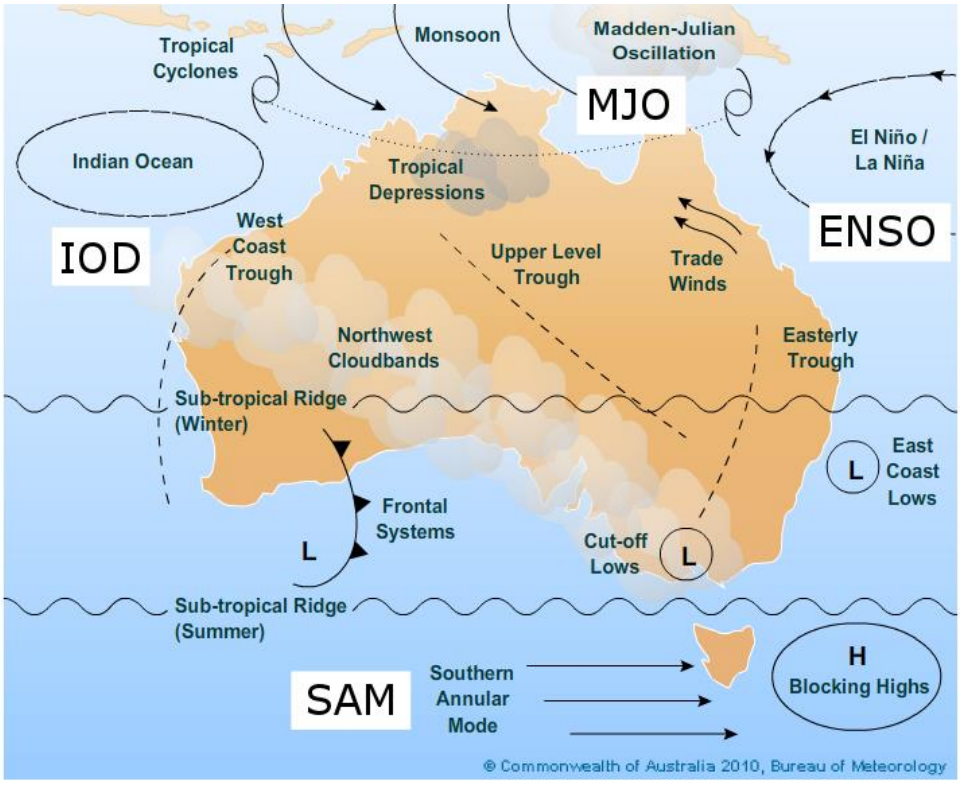

Figure 1: Main climatic drivers of the Australian continent, modified from BoMA (2017a).

The climate variability in Australia is dominated by four atmospheric systems dominating (BoMA, 2017a; CSIRO, 2015). Figure 1 displays their position along the Australian continent. The most relevant driver is the El Niño Southern Oscillation (ENSO). An El Niño event (negative ENSO) is typically accompanied by reduced rainfalls and warmer temperatures in southeast Australia and a delay in the monsoon season in the north. “La Niña” (positive ENSO) brings increased rainfalls to the whole continent, lower temperatures to the south and an earlier onset of the monsoon for the north (BoMA, 2017d). The strong influence of ENSO anomalies on rainfall patterns and the development of droughts in Australia has been reported numerous times (CSIRO, 2015; van Dijk et al., 2013; Dai, 2011; Chiew et al., 1998). Often, ENSO anomalies are temporarily coupled to anomalies in the Indian Ocean Dipole (IOD). Active from May to November, the IOD prompts reduced seasonal rainfall over central and southern Australia but can - depending on its direction of movement - also bring above average rainfall to these regions.

The seasonal monsoon in the north is mainly determined by the Madden-Julian Oscillation (MJO), an eastward moving disturbance over the Indian and Pacific Ocean bringing heavy rainfall for 40 - 60 days to Northern Australia. Finally, the Southern Annular Mode (SAM) controls the seasonal distribution of rainfalls in southern Australia by either attracting low pressure systems from the Antarctic (in winter) or by detracting them (in summer) (CSIRO, 2015).

Often, droughts in Australia result from anomalies in either one or many of these drivers. For example, a long period of negative ENSO during the Federation drought or a negative ENSO coupled with a positive Southern Annular Mode (SAM) during the Millennium drought (Verdon-Kidd and Kiem, 2009). As much as these drivers are capable of initiating droughts they are capable of breaking them. This happened as such in 2010 when a positive ENSO coupled with a strongly negative SAM phase brought heavy rainfalls to the Murray Darling River Basin ending the Millennium drought in southeast Australia (CSIRO, 2015).

There is widespread recognition that rainfall anomalies are a key factor in the development of droughts worldwide and particularly in Australia (Kirono et al., 2011; Hannaford et al., 2011; Cai and Cowan, 2008a; Nicholls, 2004). One reason for this strong influence is that the temporal fluctuation of precipitation is higher than those of other influencing variables (Vicente-Serrano et al., 2012a). However, there is evidence that, under conditions of global warming, contributions from other factors might increase, such as high temperature and evapotranspiration rates (Vicente-Serrano et al., 2014; Teuling et al., 2013; Cai and Cowan, 2008b), low soil moisture content (Tijdeman et al., 2012; Cai et al., 2009) or low runoff (Haslinger et al., 2014; Yu et al., 2010). The question to what extent each of these additional factors will contribute to future drought events is not well understood yet (Haslinger et al., 2014).

1.3 Climate change in Australia and repercussions on the hydrosphere

Recent global warming scenarios suggest that droughts will remain a key concern for Australia within the next decades. Climate models predict a decrease in rainfall for the continent by 3 - 5% accompanied by a rise of mean temperature of 0.6 - 1.3°C by 2030 and a growing atmospheric moisture demand (CSIRO, 2015).

The confidence in climate projections for Australia varies strongly across the continent and across the different climate parameters. There is “medium to high confidence” (CSIRO, 2015) that precipitation patterns on the continent may change in the near future. Rainfall over southern and large parts of eastern Australia will likely continue to decline, especially in the cooler months (winter and autumn). In the north, mean annual rainfall might increase, however with less certainty due to high natural fluctuations. Along with the deficits in winter rainfall, snowfall in the Australian Alps will decline, especially at low altitudes, leading to an increased snow melt in the near future. Also, soil moisture and runoff will likely decrease (CSIRO, 2015; Cai et al., 2009). This will probably amplify the water scarcity in highly irrigated agricultural areas in southeastern Australia.

As a consequence, the duration, frequency and severity of droughts is projected to increase for large parts of the continent.

1.3.1 Streamflow trends in Australia

A large number of studies have investigated temporal trends in Australian streamflow data. Chiew and McMahon (1993) analyzed annual runoff series for 30 unregulated rivers and found no clear evidence for a negative trend. Potter et al. (2010) showed that from 1997 to 2006 the runoff in some parts of the Murray Darling River Basin declined by 50% compared to the long-term average, while rainfall declined by only 20%. In line, McFarlane et al. (2012) found that streamflows in Western Australia significantly declined since 1975 and that this decline was stronger than the decline in rainfall and additionally accompanied by a decline of groundwater tables. In a recent study, Zhang et al. (2016) analyzed a similar data set as provided for this thesis. They identified differing streamflow trends for the different hydro-climatic regions in Australia: in the northwest the runoff had significantly decreased since 1950, no significant trend was found for streamflows in Western

Australia, the Outback, Tasmania and northern Queensland, whereas in the southeast a significant decrease in runoff was observed.

1.3.2 Effects of temperature and evapotranspiration on streamflows

Recent efforts to quantify the effect of increased temperatures and evapotranspiration rates on streamflows were facing two questions: (1) Is there empirical evidence for a stronger decline in streamflows during droughts accompanied by heat waves in comparison to droughts accompanied by average temperatures? And (2) can this stronger decline be attributed to higher evapotranspiration rates?

Various attempts have been made to bring light to these questions (Vicente-Serrano et al., 2014; Teuling et al., 2013; Kiem and Verdon-Kidd, 2010; Chiew, McMahon 1993). At first sight, it seems logical to presume that higher evapotranspiration rates have generally a negative effect on runoff (Nicholls, 2004). However, this negative effect might be compensated by generally lower water availability, creating a "drought paradox" (Teuling et al., 2013). One challenge appears to be isolating the effect of temperature from other impact factors. This can be problematic due to i.e. human influence (damming, irrigation) (Vicente-Serrano et al., 2014; Kiem and Verdon-Kidd, 2010), highly complex interactions of multiple variables and low confidence in climate projections (van Dijk et al., 2013) or simultaneous variations in other possibly relevant variables, such as groundwater or land use (Kiem and Verdon-Kidd, 2010).

Van Dijk et al. (2013) identified a growing influence of rainfall deficiencies related to El Niño events on the severity of droughts in Australia leaving it open if and how much temperature and evapotranspiration have exacerbated the impacts of the Millennium drought. In contrast, numerous studies presented empirical evidence that high temperatures have had a strong impact on rivers in the southeast Australia (Kiem et al., 2016; Chiew et al., 2011; Yu et al., 2010; Verdon-Kidd and Kiem, 2009; Cai and Cowan, 2008a, 2008b).

Though rainfall was very low during the Millennium drought the decline in precipitation alone could not sufficiently explain the reduced inflow rates in the Murray Darling River Basin (Chiew et al., 2011). Cai and Cowan (2008b) showed that precipitation alone was unable to fully explain the fluctuations of inflow rates in the southeast. Instead there had to be a loss of water through a higher atmospheric water demand. In a further study, Cai et al. (2009) found that one key factor for the

decrease in inflow rates in the southeast was a higher sensitivity of soil moisture to precipitation in comparison to previous droughts. They suggested that a projected temperature rise of 1°C by 2030 would reduce the annual river inflow in South Australia by 15%. Kiem and Verdon-Kidd (2010) critically remarked that Cai et al. (2009) may have underestimated precedent soil moisture conditions and the decline in runoff could also be explained by others factors, i.e. increased losses to groundwater, changes in bush fire management, water management activities or a seasonal shift in rainfall intensities.

Potter and Chiew (2011) found that between 1997 and 2008 the decrease in mean annual runoff observed for many rivers in the southeast was much larger than the decrease in mean annual rainfall. They suggested that, besides the influence of temperature, seasonal rainfall deficits in autumn – an important "wetting period" in the region – might be responsible for the lower runoff. The effect of the disproportionally large decline in autumn rainfall on annual streamflow patterns has also been discussed by Zhang et al. (2016), Saft et al. (2016), van Dijk et al. (2013) and Cai and Cowan (2008a).

An influence of temperature on streamflows was also identified for other semi-arid regions in the world. Vicente-Serrano et al. (2014) showed for the Iberian Peninsula that rising evapotranspiration rates have significantly contributed to declining surface water resources in Spain and Portugal. They introduced an interesting thought on why increasing temperatures present a "new source of stress" (Vicente-Serrano et al., 2014) for the environment particularly affecting the hydrosphere: While vegetation has the ability to adapt to rainfall scarcity there is no equivalent process lowering evaporative losses from the geosphere (Vicente-Serrano et al., 2014). The impact of global warming on rivers mainly fed by water from the upper geosphere (soil moisture, surface runoff) could thus be higher than for rivers fed mainly by groundwater aquifers (Vicente-Serrano et al., 2014).

2 Data and study area

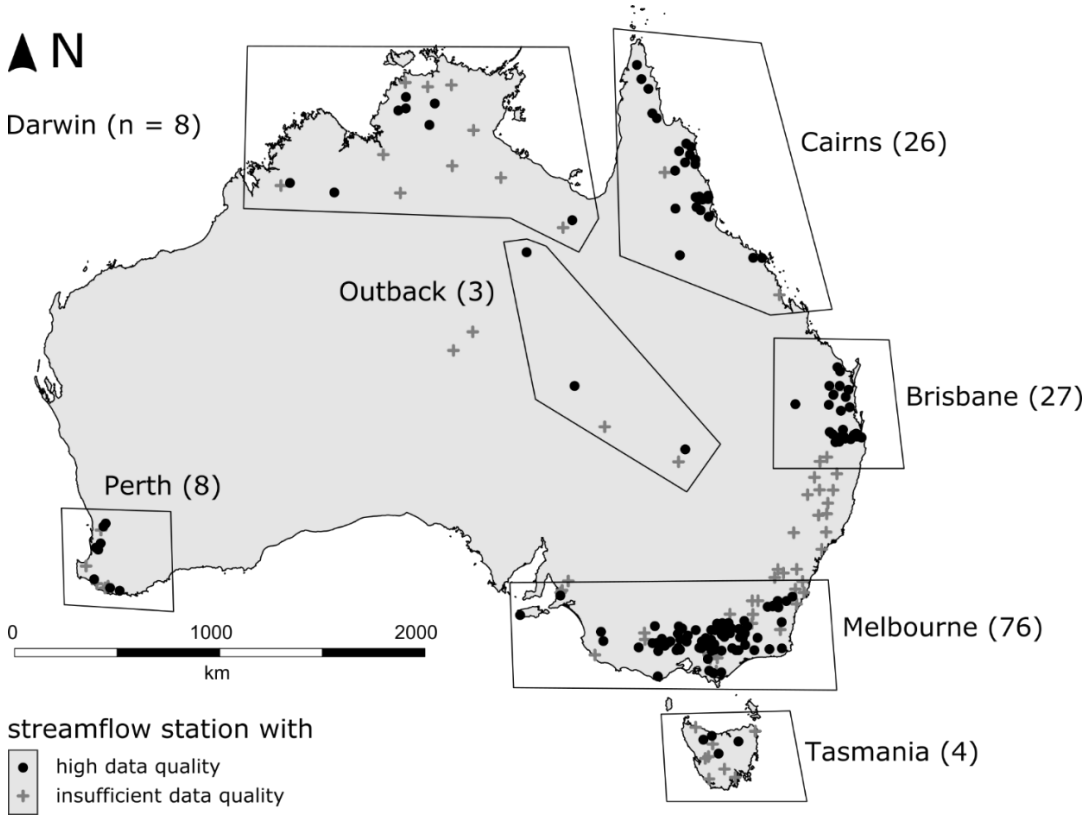

Map 1: Spatial distribution of the 222 hydrologic reference stations. Black dots: stations with high data quality (n = 152). Grey crosses: stations with insufficient data quality (n = 70, excluded from further analysis). The 152 streamflow stations were grouped in seven research regions based on regional clusters and the Koeppen Geiger climate zones (n = sample size per region).

The data set for this thesis originates from the Australian Online Climate Database (BoMA, 2017b). In total, three raw data sets were processed: (1) a data set of daily streamflow records for 222 hydrologic reference stations across Australia with varying start and ending dates from 1973 to 2014, including geographic coordinates. (2) A raster stack of mean monthly precipitation data for the Australian continent for the same time period and (3) a raster stack of mean monthly air temperature data (Tmin, Tmax) for the Australian continent also for the same time period (resolution: 5.5 x 5.5 km).

Map 1 displays the location of the 222 hydrological reference stations. The black dots symbolize stations with a sufficiently high data quality. Those stations were used for further analysis. The stations symbolized by a grey cross were excluded from further analysis. An overview on the group

size per region can also be found in Table 1. The selection criteria will be outlined in the following section.

Table 1: Overview: Amount of stations that were used for analysis (high quality) vs amount of stations that were excluded from analysis (insufficient quality) per region.

group	Melbourne	Tasmania	Perth	Brisbane	Cairns	Darwin	Outback	total
Used for analysis	76	4	8	27	26	8	3	152
Excluded from analysis	21	8	5	3	3	10	20	70

2.1 Selection criteria for streamflow data

Each daily streamflow record was flagged with a quality label indicating one of seven quality levels ranging from A ("best available data"), B ("good data") to G ("gap filled", "unreliable") (BoMA, 2017c). For the calculation of a mean monthly runoff three selection criteria were set up: (1) every month was required to have at least 28 daily records of which (2) at least 50% needed to be flagged A or B and (3) every streamflow station was required to have at least 35 years of records. This reduced the number of stations from 222 to 152 (see Table 1).

2.2 Processing of precipitation, evapotranspiration and WB data

$$PET = 0.0023 * R_a * (T + 17.8) * TR^{0.50}$$

Equation 1: Hargreaves equation to estimate the potential evapotranspiration (PET) (Hargreaves 1994). R_a is the mean monthly external radiation in MJ per m^2 and month (calculated as a function of the latitude), T is the mean monthly temperature (calculated as (Tmax + Tmin) / 2) and TR is the monthly temperature range (calculated as Tmax - Tmin).

The mean monthly precipitation value for each station was extracted from the nationwide raster using the *extract()* function from the r package 'raster' (Hijmans et al., 2016). The potential evapotranspiration (PET) was estimated using the original Hargreaves equation (Hargreaves, 1994). Hargreaves calculates the PET as a function of the minimum and maximum monthly air temperature and the latitude, as shown in Equation 1.

2.3 Climate zones in Australia

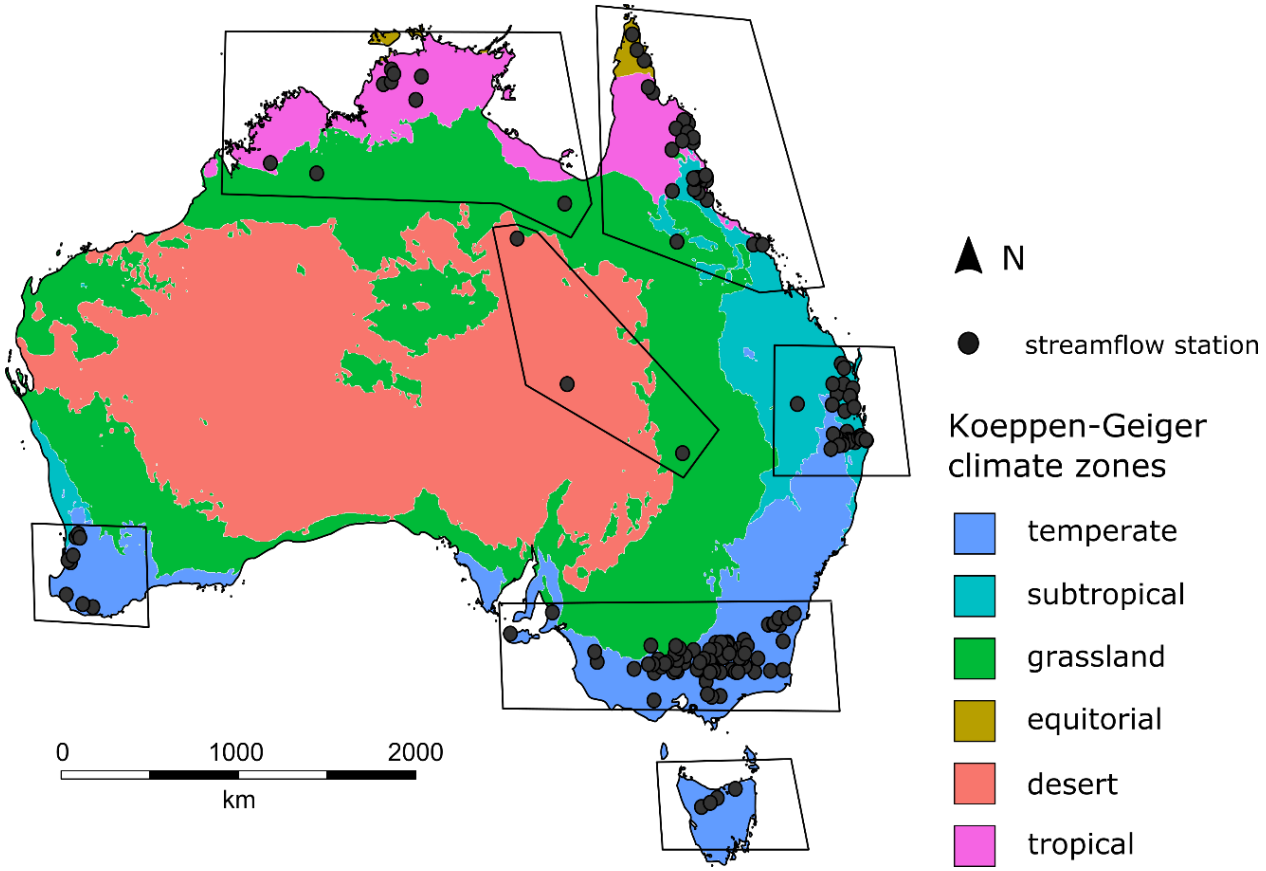

Map 2: Distribution of the streamflow stations (black dots) over the Koeppen-Geiger climate zones (Peel et al., 2007).

Table 2: Total number and proportion of stations per climate zone.

climate zone	temperate	subtropical	tropical	grassland	equatorial	desert	ttl
total number	99	25	20	3	3	2	152
percentage	65%	16%	13%	2%	2%	1%	100%

Map 2 displays the distribution of the 152 high quality stations across the six climate zones. Table 2 shows the total number of stations per climate zones and their proportion on the complete data set of 152 stations. It can be seen that Australia is a climatically highly variable continent. It spans over six main climate zones from the tropical to equatorial north at 10°S to the temperate south at 43°S.

The north encounters monsoonal rainfalls in summer with mean annual temperatures of 27°C to 30°C. Its water balance is precipitation dominated and negative from April to November due to high evapotranspiration rates throughout the year. The southern coast receives constant rainfalls which are however prone to high interannual and seasonal variability. The annual mean temperatures in the southeast ranges from 12°C in Tasmania to 15°C in northern Victoria.

In the recent decades, precipitation in Australia has shifted from southeast to northwest. The tropical northwest (Darwin) has seen an increase in mean rainfall of 30 - 50 mm per decade also affecting large parts of the southern inland. In the southeast (Melbourne, Tasmania), the southwest (Perth) and along the eastern coastline (Brisbane, Cairns) mean rainfalls decreased by 30 to 50 mm per decade. A map displaying this trend can be found in Annex 1.

2.4 Southeast Australia (Melbourne region)

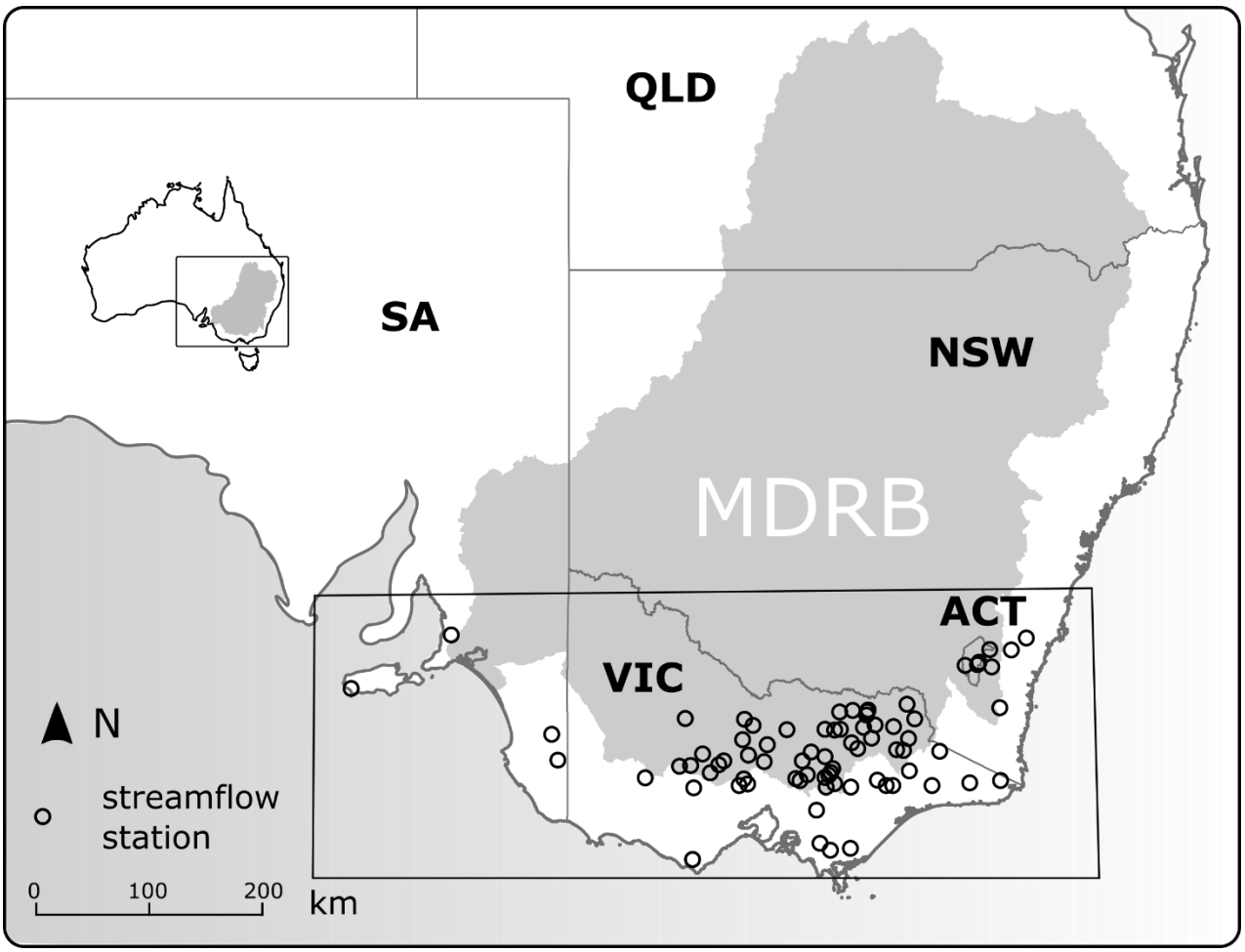

Map 3: Location of the 76 streamflow stations of the Melbourne region. The stations spread over four federal states (South Australia (SA), Victoria (VIC), New South Wales (NSW) and the Australia capital territory (ACT)). A majority of stations are located in the Murray-Darling River Basin (MDRB).

The streamflow stations in southeast Australia (Melbourne region) form the largest group in this thesis (76 stations). As shown in Map 3, the 76 stations span over four federal states. The majority of stations are located in the state of Victoria (VIC), a large proportion of rivers in the Melbourne region originate in the Murray-Darling River basin, Australia's most important hydrological basin.

The climate in southeast Australia is temperate. Summers are usually mild to hot, followed by a pronounced wetting period in late autumn and winter. The annual mean temperature is 15.2°C

(1961 - 1990). From 1970 and 2016, the mean temperature increased by 0.05 - 0.4 °C per decade while the mean annual rainfall declined by 5 - 40mm per decade (data from BoMA (2017b)).

The MDRB receives relatively little rainfall (annual mean: 465 mm, 1961 – 1990, BoMA (2017b)). Only 4% of the annual rainfall becomes runoff while 94% evaporates or transpires (ABoS, 2008). Many rivers in the region are ephemeral and only watered in the cooler months. Although the region is relatively dry, the gross value of the agricultural production (GVAP) in the MDRB accounts for ~39% of the total Australian GVAP (ABoS, 2008). As a consequence, irrigation and water security are crucial for the local agricultural industry, especially in Victoria where the largest irrigation district in the MDRB can be found.

The state of Victoria has about 450,000 dams with a total storage capacity of 13,400,000 megalitres (DEPI 2014). Their main purposes are water supply for urban and irrigated areas and hydropower generation (DEPI 2014). The question if and how much water can be taken from to rivers without damaging the environmental balance is harshly debated. At least in one case, inappropriate damming strategies were suspected to have caused a local streamflow drought in 2011 (SMH, 2011).

2.4.1 Hydroclimate at sample station: Murrindindi River

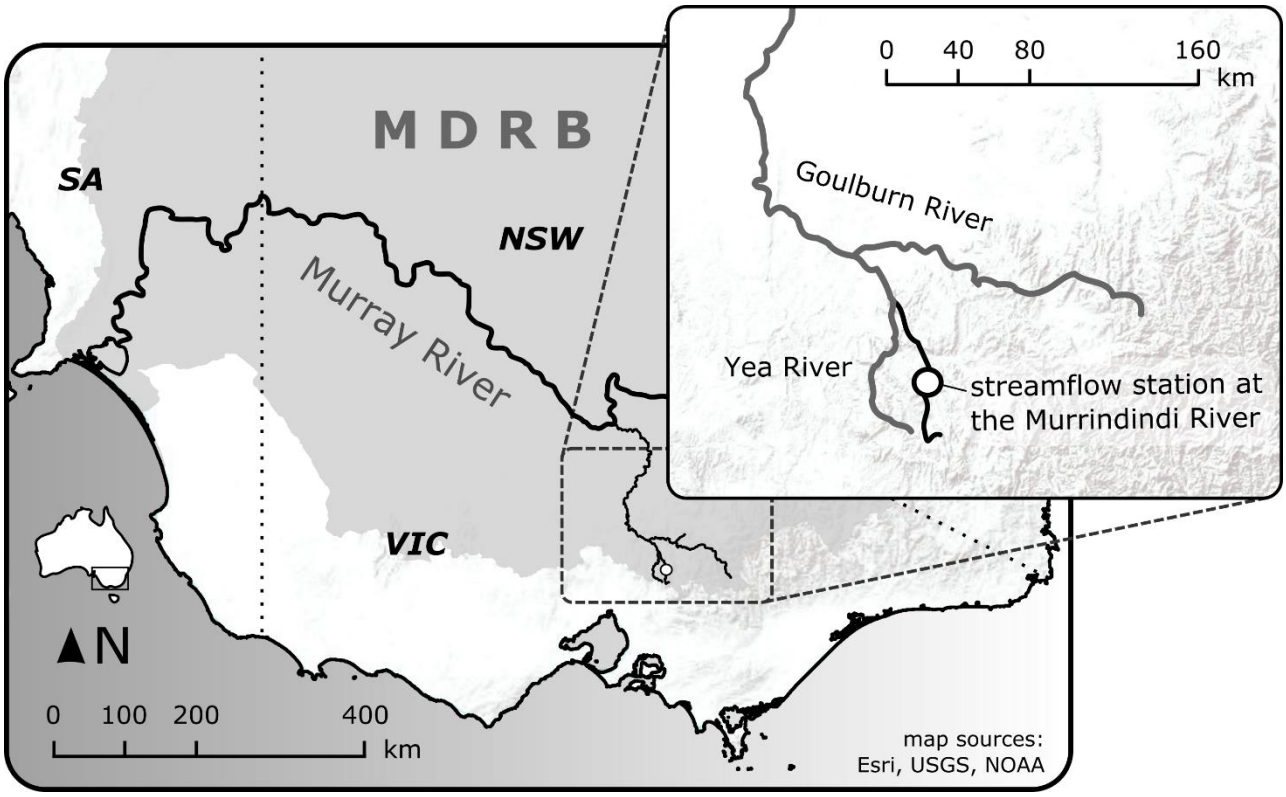

Map 4: Location of the Murrindindi River and its reference station (white circle, zoomed map on right) in southeast Australia. The station lies at an altitude of 335 m above sea level, on the southwestern side of the Great Dividing Range.

Table 3: Basic statistics of the Murrindindi streamflow station (data from BoMA (2017b)). Monthly runoff, annual runoff, maximum air temperature, minimum air temperature and precipitation for the years 1975 to 2014.

	mean	min	q25	q75	max
Monthly runoff	39 mm	5 mm	22 mm	50 mm	186 mm
Annual runoff	461 mm	182 mm	372 mm	541 mm	885 mm
Mean Monthly Tmax	18.2°C	8.8°C	13.2°C	23.3°C	29.9°C
Mean Monthly Tmin	7.6°C	0.8 °C	4.7°C	10.4°C	14.9°C
Precipitation	89 mm	0 mm	49 mm	123 mm	259 mm

The Murrindindi River is a 29 km long perennial river that springs 100 km northeast of Melbourne in the Victorian Alps (MDRB). It rises at an altitude of 1010m in the southwestern mountains of the

Great Dividing Range and flows into the Yea River before finally draining into the Murray River. The station lies at an altitude of 335 m above sea level and receives continuous rainfalls throughout the year. The water year lasts from March to February.

As shown in Table 3, the Murrindindi even carried water during the Millennium drought (lowest: monthly runoff 5mm, recorded in February 2007). The runoff is highest from late winter to early spring and lowest in late summer. The pardé coefficients for the Murrindindi River can be found in the digital annex of this thesis.

The Murrindindi was chosen for a deeper analysis in part II of the thesis because the river is usually well watered throughout the year and does not fall completely dry. This guaranteed full data availability for the seasonal analysis.

3 Methods

Table 4: Drought severity classification based on indicator ranges and their occurrence probability.

range	drought level	probability
indicator ≥ 0.0	No drought	50.0%
indicator < 0.0	Drought	50.0%
-1.0 ≤ indicator < -0.0	Mild drought	34.1%
-1.5 ≤ indicator < -1.0	Moderate	9.2%
-2.0 ≤ indicator < -1.0	Severe	4.4%
indicator ≤ -2.5	Extreme	2.3%

3.1 Part I: Characterizing droughts through indicators

Drought indicators are an essential instrument in drought monitoring all over the world. Droughts indicator enable the classification of different severity and occurrence probability levels (Table 4). Numerous indicators types have been developed and tested in their ability to identify the severity, duration and spatial extent of different types of droughts (Bachmair et al., 2016; Eilertz, 2013; Dai, 2011; Vicente-Serrano et al., 2012b; Vicente-Serrano et al., 2012a; Dai, 2011; Mpelasoka et al., 2008).

The Palmer drought severity index (PDSI) (Palmer, 1965) and its various subtypes process precipitation, temperature and soil moisture data and is often used to quantify the relative dryness of a region (Eilertz, 2013; Vicente-Serrano et al., 2012a). Despite its widespread utilization the PDSI has several shortcomings, for example, limited explanatory power when applied on climate zones outside the US (Vicente-Serrano et al., 2012a), i.e. in Australia (Mpelasoka et al., 2008), or on future drought scenarios (Kiem et al., 2016). The Australian Bureau of Meteorology has based its drought forecast system on accumulated rainfall percentiles to define the severity of droughts (WMO, 2006). In the US, the computed Soil Moisture index (CSM) is a common indicator for agricultural and hydrological droughts (Dai, 2011).

McKee et al. (1993) introduced the concept of the Standardized Precipitation Index (SPI), an indicator solely based on precipitation. One main purpose of the SPI was to develop an indicator that accounts for the major role of precipitation in the occurrence of droughts. Where precipitation

is lacking multiple water resources are affected at various time steps, i.e. soil moisture content on the short term and groundwater storages on the long term (WMO, 2012). To account for this aspect, the SPI can be calculated for different accumulation periods (McKee et al., 1993). These different time scales may be used to monitor drought impacts on different water resources in the hydrological cycle (Vicente-Serrano and López-Moreno, 2005).

Though the SPI has become a "standard tool" (van Lanen et al., 2016) of drought research, both worldwide (Haslinger et al., 2014; Lorenzo-Lacruz et al., 2013) and for Australia (Deo et al., 2016; Rahmat et al., 2015; WMO, 2006) it has often been criticized for not reflecting the increasing influence of temperature on droughts (Vicente-Serrano et al., 2012a; 2010). To bridge this gap Vicente-Serrano et al. (2010) developed a refined version of the SPI, the Standardized Precipitation and Evapotranspiration Index (SPEI). The SPEI is based on the water balance and considers, additionally to precipitation, water losses through evapotranspiration (Blauhut et al., 2015).

The principle of standardizing a time series can be applied on various climate variables. The Standardized Streamflow Index (SSI), for example, represents the standardized runoff of a river and enables the comparison of hydrological streamflow conditions over space and time (Lorenzo-Lacruz et al., 2013; Vicente-Serrano et al., 2012b).

3.1.1 Correlating meteorological and hydrological drought indicators

The explanatory power of meteorological drought indicators to predict hydrological anomalies has been investigated numerous times (Barker et al., 2016; Vicente-Serrano et al., 2014; Lorenzo-Lacruz et al., 2013; Eilertz, 2013). Comparative tests have shown that SPEI often yields better results than SPI (Bachmair et al., 2016), i.e. by providing higher maximum correlations with SSI (Vicente-Serrano et al., 2014) or by identifying low flow events more accurately (Haslinger et al., 2014).

In semiarid regions on the Iberian Peninsula, SPEI provided distinctly higher correlations than SPI (Vicente-Serrano et al., 2014; 2012a). Furthermore, SPEI tends to be most superior to SPI in late spring and summer when the atmospheric water demand is highest and least superior in winter when the atmospheric water demand is lowest (Vicente-Serrano et al., 2012a). Nevertheless, the performance differences between SPI and SPEI can be very small for some climate zones (Eilertz, 2013; Vicente-Serrano et al., 2012a). In moist areas, correlation strengths can be lower and the

difference between both indicators smaller, whereas in semi-arid to arid regions correlation strength is higher and the superiority of SPEI over SPI more pronounced (Li et al., 2015).

A higher correlation of SPEI versus SSI in comparison to SPI versus SSI indicates an influence of evapotranspiration on the variability of streamflow droughts (Vicente-Serrano et al., 2014). Though, this seasonality can be masked, i.e. by river regulation (dams, reservoirs) or water extraction for irrigation (Vicente-Serrano et al., 2014; Lorenzo-Lacruz et al., 2013).

3.1.2 The role of accumulation periods

In this thesis, the term “response time” is used as a synonym for to the accumulation period of SPI/SPEI at which the correlation between SSI and SPI/SPEI is highest.

Response times may be regionally highly variable, i.e. due to differences in geology, topography and land cover (López-Moreno et al., 2013), seasonal and interannual rainfall patterns or aquifer characteristics (Barker et al., 2016). Also, river regulation and damming operations may have a strong impact on response times. Lorenzo-Lacruz et al. (2013) investigated the influence of river regulation on response times and found significant differences between regulated and unregulated streamflows.

3.2 Part I: Calculating the indicator: SPI, SPEI and SSI

Standardized drought indices are calculated by converting a time series into a standardized normal distribution (McKee et al., 1993). First, a probability density function is fitted to a frequency distribution, then the probabilities from this function are converted to a standard normal distribution (Li et al., 2015). This enables the comparison and correlation of different standardized indicators over time and space. The indicators were calculated using r package “SCI” (Gudmundsson and Stagge, 2016).

Stagge et al. (2015) examined the influence of different distributions on the performance of SPI and SPEI and recommend the gamma distribution for SPI and SSI, and the generalized extreme value distribution (GenEV) for SPEI. However, similarly low Shapiro–Wilk rejection frequencies as with the GenEV can be reached using the generalized logistic distribution (GenLOG). Herein, GenLOG was

preferred for SPEI due to a lower amount of missing values (NA) in the final output. Table 5 provides an overview on the distributions used for the calculation of SPI, SPEI and SSI in this thesis.

Table 5: Distributions and accumulation periods for SPI, SPEI and SSI.

indicator	accumulation periods	distribution for normalization
SPI	1 – 24 months	GenLOG
SPEI	1 – 24 months	gamma
SSI	1 month	gamma

3.3 Part I: Correlating meteorological and hydrological signals

In order to investigate the explanatory power of SPI and SPEI to predict streamflow droughts, Spearman rank correlation coefficients and significance levels were calculated for all SPI/SPEI accumulation periods versus the SSI. This was done (1) for the complete annual time series and (2) for seasonal time series separately.

One commonly reported problem when correlation meteorological and hydrological time series is differentiating correlation effects originating from wet periods from correlation effects originating from dry periods. Subdividing the data set to only negative indicator values can lead to a noticeable loss of significance and correlations strength (Eilertz, 2013). To this end, this thesis uses the same approach as Haslinger et al. (2014) by subdividing the data set by seasons. By doing so the sample size could kept stable.

3.4 Part II: Low flow model and linear trend analysis

A low flow event was defined as moment at which the monthly runoff drops below the 10th monthly percentile. Months in which the streamflow fell below the 10th percentile were flagged "$flow_{10}$". Months in which the 10th percentile was exceeded were named $flow_{>10}$. The result was a binary vector ("low flow") containing 1 for months with $flow_{10}$ and 0 for months with $flow_{>10}$.

In humid areas - where droughts are by definition exceptional - the proportion between the total amount of $flow_{10}$ and total number of $flow_{>10}$ events is, ideally, 1/9. However, in areas where dried out river beds occur naturally and regularly, this proportion can easily be higher, especially where missing values decrease the total number of events. To ensure that the number of both $flow_{10}$ and $flow_{>10}$ events is large enough, only stations were respected for modelling where the number of $flow_{10}$ events added up to more than 10% and less than 90% of the total number of events.

Many previous approaches have related the occurrence of environmental hazards to environmental variables using a binary logistic regression model (Blauhut et al., 2015; Gudmundsson et al., 2014; Chou et al., 1993). The occurrence likelihood of a $flow_{10}$ event can be described using a logistic regression as:

$$\log\left(\frac{likelihood\ flow_{10}}{1 - likelihood\ flow_{10}}\right) = \alpha + \beta * SPEI$$

Equation 2: Binary logistic regression model, logit transformation. With $flow_{10}$ = the binary vector (1/0) indicating a $flow_{10}$ event (1) or no $flow_{10}$ event (0), α and β = model parameters defining the shape of the likelihood curve and SPEI = an SPEI time series.

The likelihood of $flow_{10}$ occurrence in percentage can then be described as:

$$likelihood\ flow_{10}\ (\%) = \left(\frac{e^{\alpha+\beta*SPEI}}{1 + e^{\alpha+\beta*SPEI}}\right)$$

Equation 3: Binary logistic regression model, percentage transformation

The probability of low flow occurrence depending on SPEI can indirectly also be interpreted from Equation 2 that describes the probability as a value between 0 (0% likelihood of occurrence) and 1 (100% likelihood of occurrence) (Blauhut et al., 2016).

The accuracy of the model was assessed using the area (AUC) under the relative operating characteristics (ROC) curve (Blauhut et al., 2015; Gudmundsson et al., 2014; Mason and Graham

2002; Peterson and Birdsall 1953). For a binary logistic regression model, the ROC curve describes the relation between correctly identified events (hit rate, sensitivity) and incorrectly identified non-events (false alarm rate, specificity) (Mason and Graham 2002). The AUC is simply the integral of the ROC curve with an AUC of 1 implying a perfect model and any AUC < 0.5 a model whose output is superior to randomness. (Blauhut et al., 2015; Mason and Graham 2002).

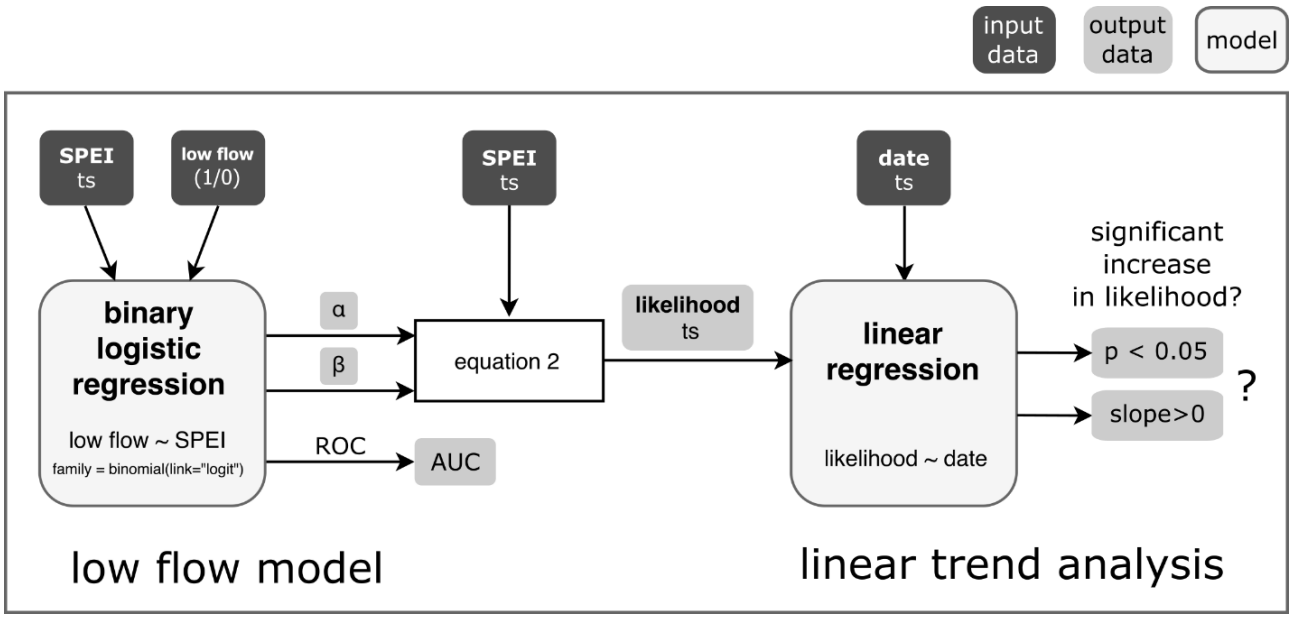

Figure 2: Working process for part II of the thesis: from low flow model to linear trend analysis. "ts" = time series.

Figure 2 displays the working process for part II of the thesis. The binary logistic regression model is fed with a continuous SPEI time series and a binary low flow vector (1 = $flow_{10}$, 0 = $flow_{>10}$).

With the help of Equation 3 the likelihood is calculated using the model parameter α and β and the SPEI time series with the highest AUC. Finally, the development of the modelled likelihood over time was assessed in a linear regression to check if the likelihood of $flow_{10}$ events significantly ($p < 0.05$) increased (slope > 0) over time. For AUC quality levels see Table 6.

Table 6: Quality levels and their AUC ranges. The AUC is used to assess the goodness of fit of the different SPEI time series in the binary regression model.

AUC	quality level
$0.9 \leq AUC < 1.0$	excellent
$0.8 \leq AUC < 0.9$	good
$0.7 \leq AUC < 0.8$	moderate
$0.6 \leq AUC < 0.7$	poor
$AUC < 0.6$	insufficient

4 Results

4.1 Part I: All-year indicator performance

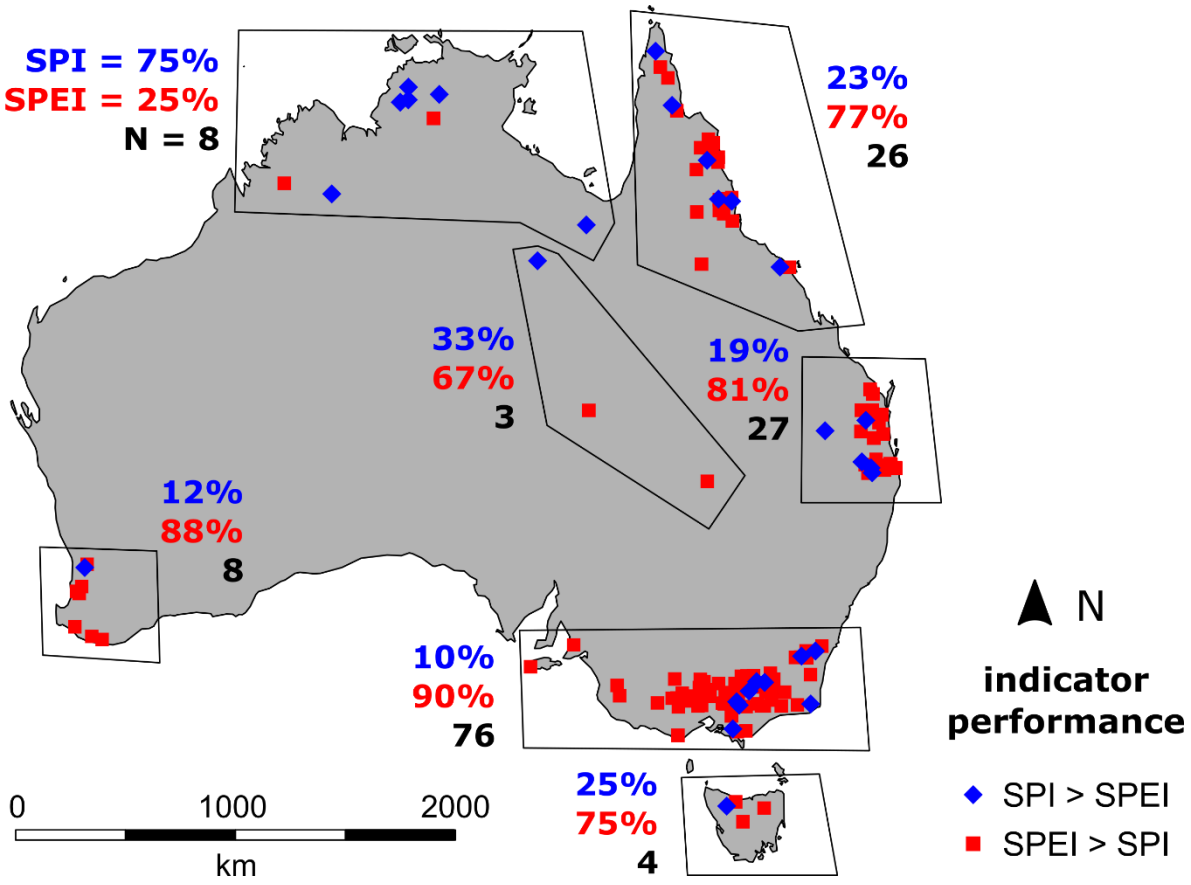

Map 5: Indicator with the highest maximum correlation with SSI (all-year). Blue: where SPI outperforms SPEI (SPI_{maxcor} > $SPEI_{maxcor}$), red: where SPEI outperforms SPI ($SPEI_{maxcor}$ > SPI_{maxcor}).

Map 5 displays the spatial performance of SPEI (red) and SPI (blue) over the Australian continent. It can be seen that SPEI is overall the better all-year indicator for large parts of the continent (82% red vs 18% blue in total). In 6 of 7 regions, the number of SPEI stations is distinctly higher than the number of SPI stations, especially in southern temperate zones (i.e. Melbourne: 90% SPEI, 10% SPI). Towards the equatorial northeast, the superiority of SPEI is fading and the number of SPI stations increases. In the tropical to equatorial north (Cairns and Darwin), the number of SPI stations is somewhat comparable to the number of SPEI stations, in the far northwest it is even higher (i.e. Darwin: 75% SPI, 25% SPEI).

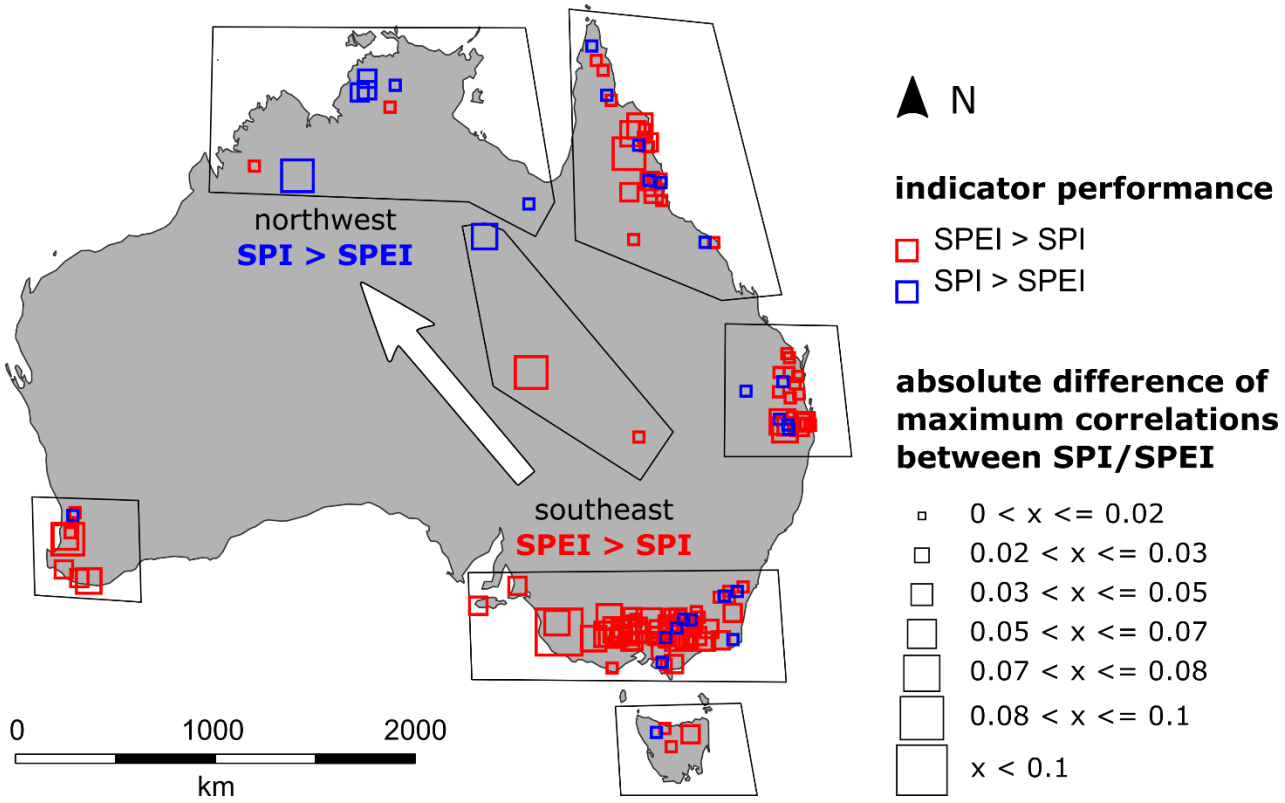

Map 6: Performance differences between SPI (blue) and SPEI (red). The square size indicates the absolute difference in maximum correlation strength between both indicators. The arrow indicates the direction of a general trend from a superiority of SPEI in the southeast to a superiority of SPI in the northwest.

Map 6 displays the absolute differences in maximum correlations of SPI and SPEI. By looking at the square size it can be seen that the superiority of SPEI in the south is relatively distinct. In the southeast and southwest, SPEI is clearly superior to SPI. This superiority is strongest in Melbourne region. Towards the northwest, the superiority of SPEI declines. In the Darwin region, SPI is superior to SPEI. The absolute differences between both indicators are rather small (for example, at 75% of all stations less than 0.025 rho, max: 0.101).

A detailed summary is presented in the following Figure 3. This figure summarizes a subsection of the results presented in the Map 5Map 6 by showing boxplots of the differences between SPI_{maxcor} and $SPEI_{maxcor}$ for the stations in Darwin (northwest), Brisbane (east) and Melbourne (southeast). It can be seen again that SPEI is superior in the southeast (Melbourne) and SPI is superior in the northwest (Darwin). With the exception of four outliers in the data sets the absolute differences between SPI and SPEI are smaller than 0.05 rho.

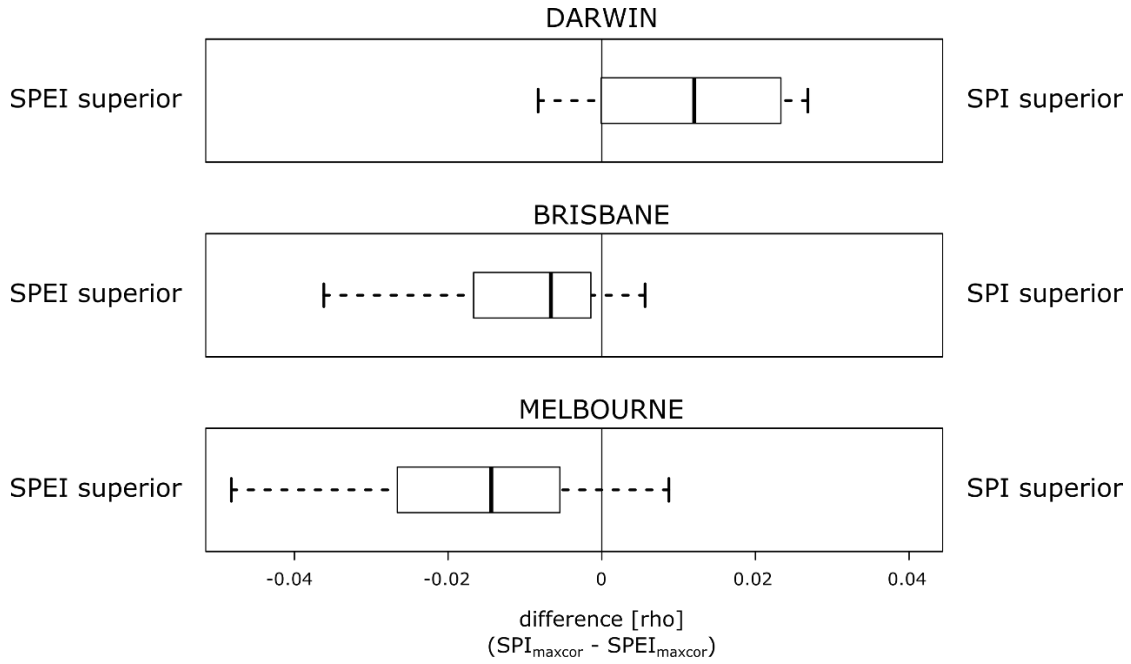

Figure 3: Boxplots showing the absolute difference between SPI_{maxcor} and $SPEI_{maxcor}$ for the stations in Darwin (northwest), Brisbane (east) and Melbourne (southeast).

Table 7: Basic statistics of maximum correlations of SPEI and SPI for the complete data set (continental) and for two selected regions in the south (Melbourne) and north (Cairns). N = sample size, q25 = 25% quantile, q75 = 75% quantile, max diff = maximum absolute difference between both indicator.

region	indicator	N	mean	median	min	q25	q75	max	max diff
Australia	SPEI	152	0.70	0.73	0.24	0.64	0.8	0.86	0.1
	SPI		0.68	0.71	0.25	0.63	0.78	0.85	
Cairns	SPEI	26	0.62	0.65	0.32	0.58	0.68	0.77	0.06
	SPI		0.61	0.63	0.32	0.57	0.67	0.76	
Melbourne	SPEI	76	0.75	0.78	0.29	0.73	0.82	0.86	0.1
	SPI		0.74	0.77	0.25	0.71	0.8	0.85	

As shown in Table 7, SPEI provides higher correlations both on the continental and on a regional scale. SPEI outperforms SPI both at stations with low correlation strengths and for stations with higher correlations strengths. Also all SPEI medians and maximums are higher than their SPI equivalents.

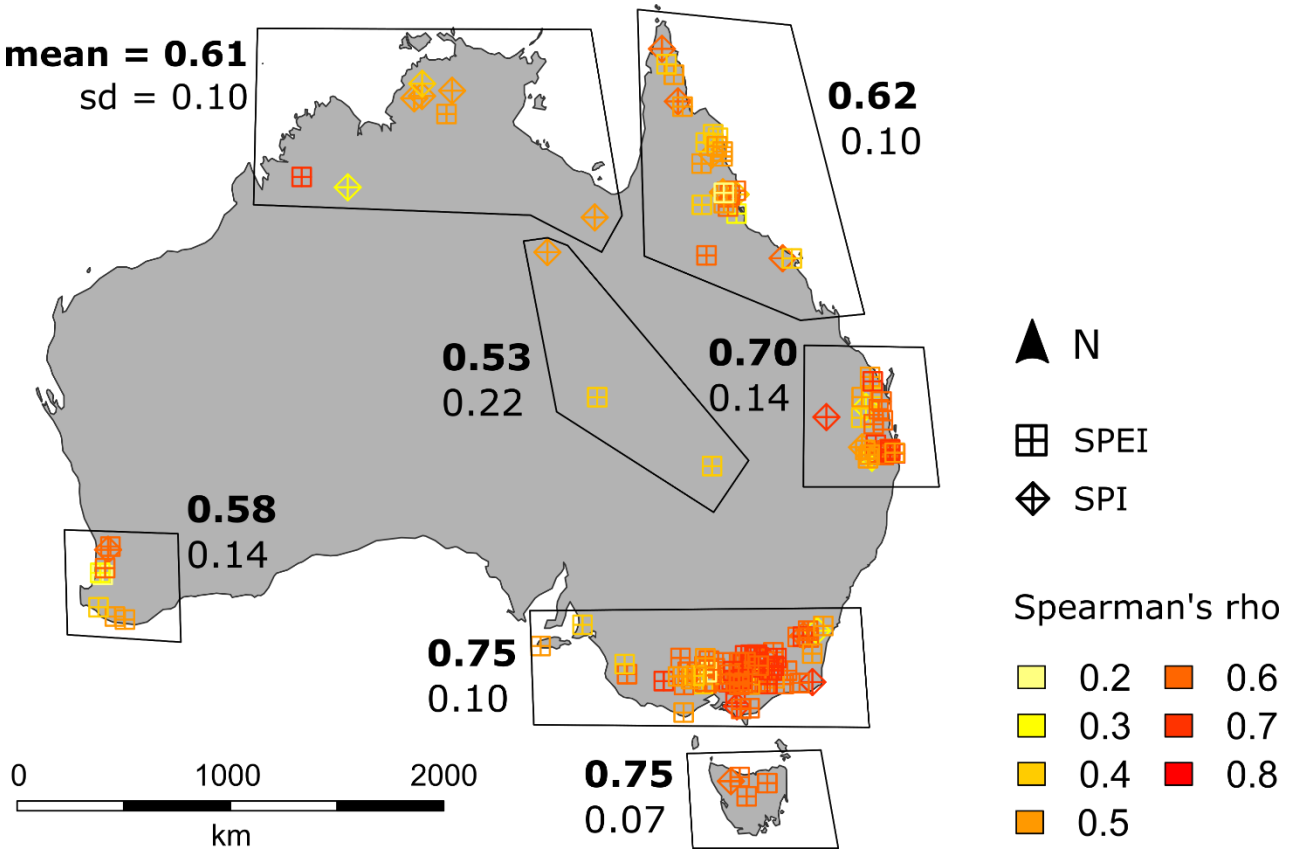

Map 7: Maximum all-year correlation strength of SPI/SPEI vs SSI. The values represent maximum correlations of the superior indicator.

Map 7 displays the maximum all-year correlation of the superior indicator to the SSI for all 152 stations. The map shows that the correlation strength varies both on the continental and on the regional scale. In average, maximum correlations are highest for the Melbourne region (mean rho = 0.75), northern Tasmania (mean rho = 0.75) and some selected stations in the Brisbane region. Towards the north, the mean correlation strength declines (i.e. Darwin: mean rho = 0.61). In the tropical/equatorial zones (Darwin, Cairns), Spearman's rho does not exceed 0.76. Contrary, in the temperate zones of the east coast (Melbourne and Tasmania), 60% of all stations (48 of 80) show a correlation > 0.76. In comparison to the other temperate regions (Melbourne, Tasmania), the correlation strength in Perth (mean = 0.58) is relatively low. Also the variability is higher there (sd = 0.14).

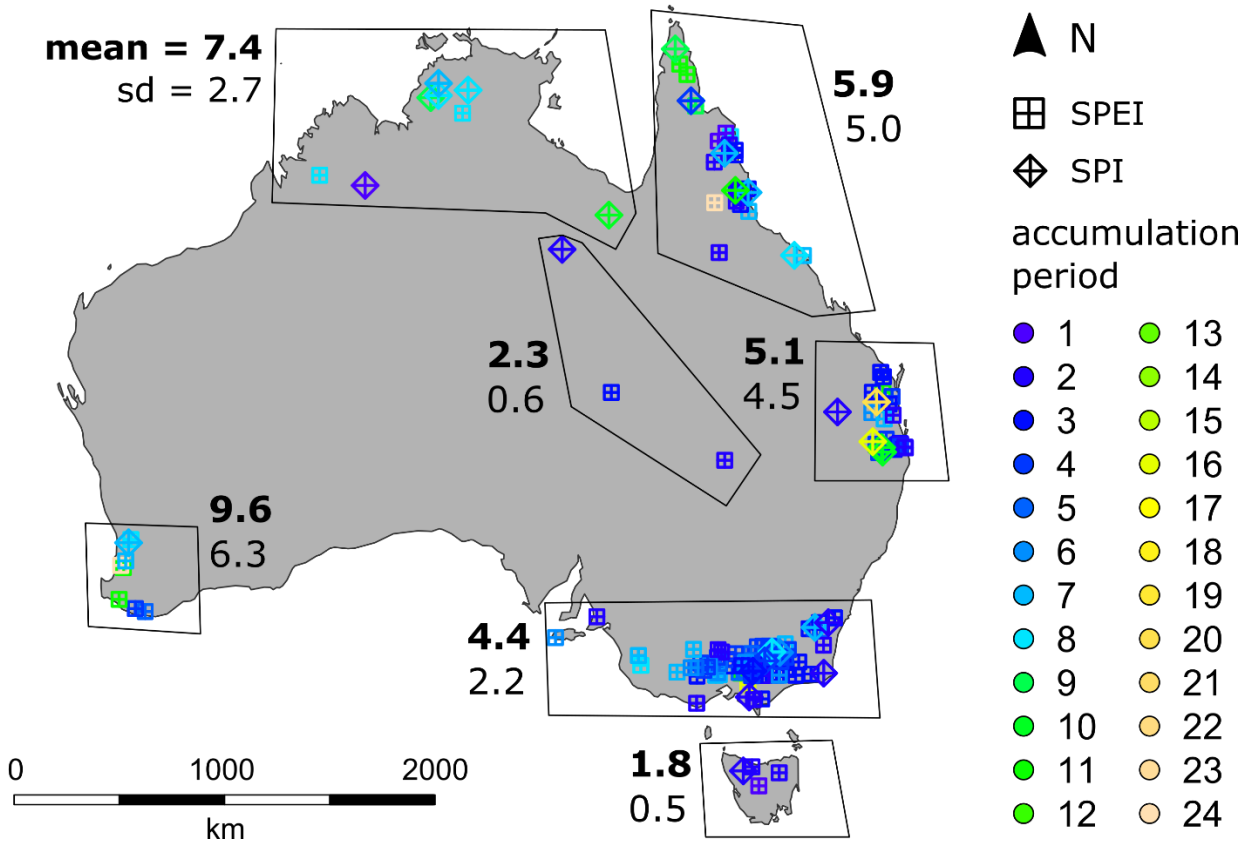

Map 8: Accumulation period with highest SPI_{maxcor}/$SPEI_{maxcor}$ (response times).

Map 8 displays the accumulation period at which the highest all-year correlation with the SSI is reached. The map shows that the response times of the stations vary strongly among the research regions. In general, response times increase from southeast to northwest (c.f. mean Tasmania: 1.8 months, mean Darwin: 7.4 months). In the southeast (Melbourne, Tasmania), short accumulation periods are most abundant, in Tasmania: 1 - 2 months for 100% of all stations, in Melbourne: 1 - 4 months for 67% of all stations.

Northwards, longer response times become more abundant. Also the variability increases. For Cairns and Brisbane, response times range from very short (Cairns: 1 month, Brisbane: 2 months) to very long (Cairns: 24 month, Brisbane: 20 months). In Darwin, 88% of the stations show maxima at 7 to 11 months.

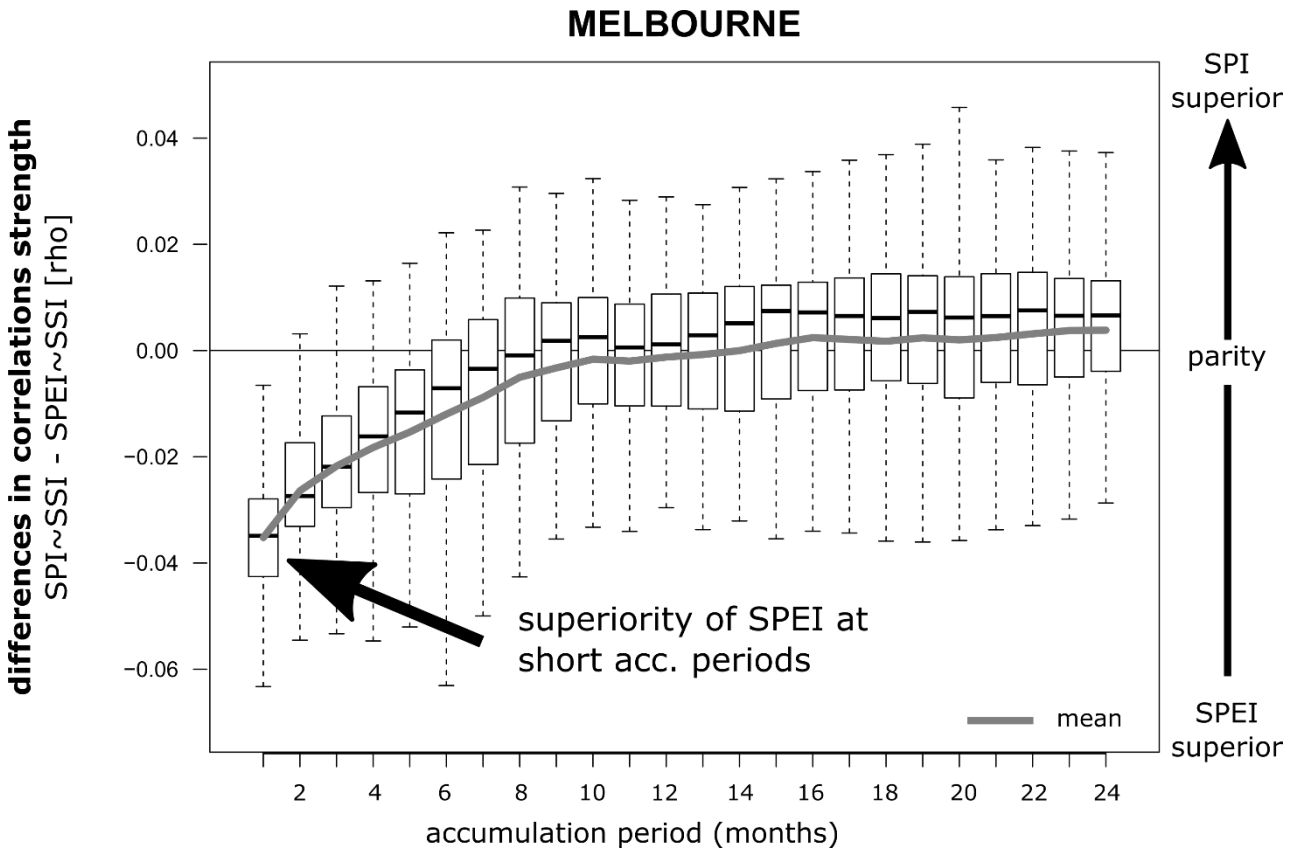

Figure 4: Boxplots: Differences in annual correlation strength (SPI – SPEI) per accumulation period for the stations in the Melbourne region. Y-axis: positive values = SPI superior, negative values = SPEI superior. Outliers are not shown.

Figure 4 shows the differences in annual correlation strength between SPI and SPEI per accumulation period for the stations in the Melbourne region. On the y-axis, negative values indicate a superiority of SPEI over SPI and, vice versa, positive values indicate a superiority of SPI over SPEI. It can be seen that in southeast Australia the performance differences between SPI and SPEI vary depending on the different accumulation periods. The largest difference between SPI and SPEI is observed at short accumulation periods (1 to 8 months). Here, SPEI is most superior to SPI. For medium to long accumulation periods (9 to 24 months) both indices provide similar correlation strengths.

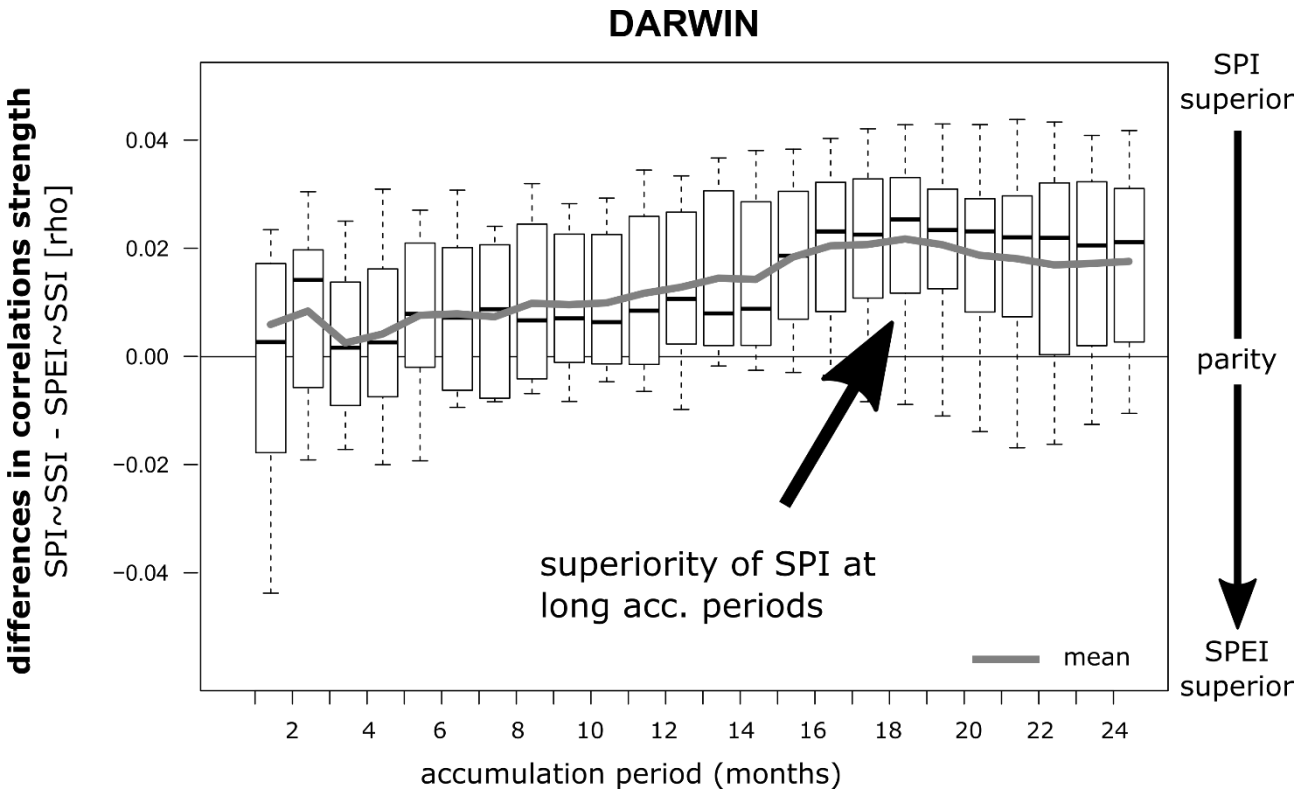

Figure 5: Boxplots: Differences in annual correlation strength (SPI~SSI – SPEI~SSI) per accumulation period for the stations in the Melbourne region. Y-axis: positive values = SPI superior, negative values = SPEI superior. Outliers are not shown.

Figure 5 shows the differences in annual correlation strength between SPI and SPEI per accumulation period for the stations in the Darwin region. For the y-axis, the same principle applies as in Figure 4. It can be seen that, in the tropical northwest, the performance differences between SPI and SPEI differ strongly from the results in Figure 4. Here, SPI performs better across all accumulations periods (mean line always positive). The superiority of SPI is most pronounced at medium to long accumulation periods (15 to 24 months, see arrow). (Although the absolute differences are in average relative small, < 0.03).

SUMMARY: RESULTS OF ALL-YEAR CORRELATION ANALYSIS

Analyzing annual correlations for the continent revealed a trend from the temperate southeast to the tropical-equatorial northwest. In southeast Australia, SPEI is distinctly superior to SPI and mainly short accumulation periods (2 – 4 months) provide high maximum correlations with SSI (i.e., median Melbourne = 0.78). Towards northwest, the superiority of SPEI is fading. Response times to SPI/SPEI increase and become more variable (peaks at 1 - 3 months and 8 - 9 months) and the overall correlation strength to SSI declines (i.e., median Darwin = 0.64).

The stations around Perth and in the Outback fit to the described trend only to some extent: In Perth, SPEI is clearly superior to SPI, however the overall correlations with SSI are the lowest of all temperate regions. The response times are variable with 2 stations showing quick responses (3 months), 3 stations medium (12 – 16 months) and 3 long responses (22 - 24 months). In the outback, SPEI is superior, too, however correlations do not show a strong northward increase and response times remain short (2 – 3 months) also for the most northern stations.

4.2 Part I: Seasonal evolution of SPEI correlation strength and response times

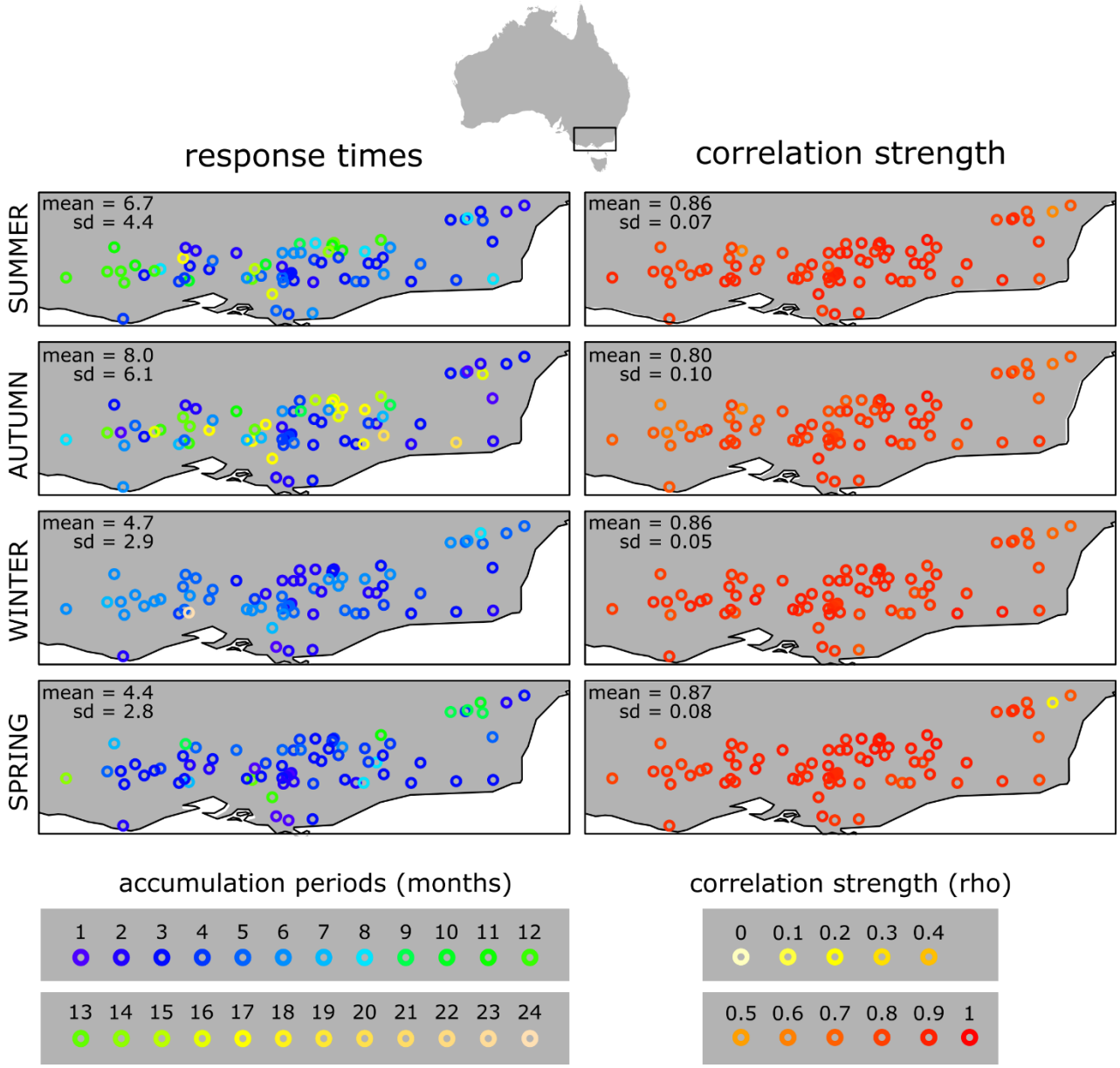

Figure 6: Response times (SPEI n, left) and maximum correlation strength (Spearman's rho, right) for selected stations of the Melbourne region, by season. The values represent accumulation period and correlation strength from the month in which the correlation was highest for the specific season, i.e. for station ID 1, "summer": December, as: $SPEI_{maxcor\_ID1\_DECEMBER}$ > $SPEI_{maxcor\_ID1\_FEBRUARY}$ > $SPEI_{maxcor\_ID1\_JANUARY}$.

Figure 6 displays the results of the seasonal correlation of SPEI versus SSI for stations in the Melbourne region. The maps on the right show that the correlation strength remains relatively

stable over all seasons (sd: 0.05 - 0.10). SPEI provides high correlations both during the high flow season in winter ($mean_{winter}$ = 0.86) and during the low flow season summer ($mean_{summer}$ = 0.86). In autumn, the mean maximum correlation is lower ($mean_{autumn}$ = 0.80). The overall seasonal fluctuations of correlation strengths are small.

In contrast to that, Figure 6 (left) shows a high seasonal variability in the response times. In winter, a clear majority (92%) of the stations show quick responses to the meteorological signal (shorter than 6 months). From spring to autumn, the number of stations with long responses (> 6 months) increases, to a maximum of 50% in autumn. Also the regional variability rises from spring to autumn (the seasonal coefficient of variation (sd/mean) is highest in autumn, 0.76). In winter the response times in the region are homogeneously short. From spring to autumn, the variability increases, with some stations showing quick responses (2 - 6 months) and some stations showing medium to long responses (12 - 16 months, 20 - 24 months).

4.3 Part II: Low flow model

4.3.1 Example: Murrindindi River

LOGISTIC REGRESSION MODEL FOR MURRINDINDI RIVER

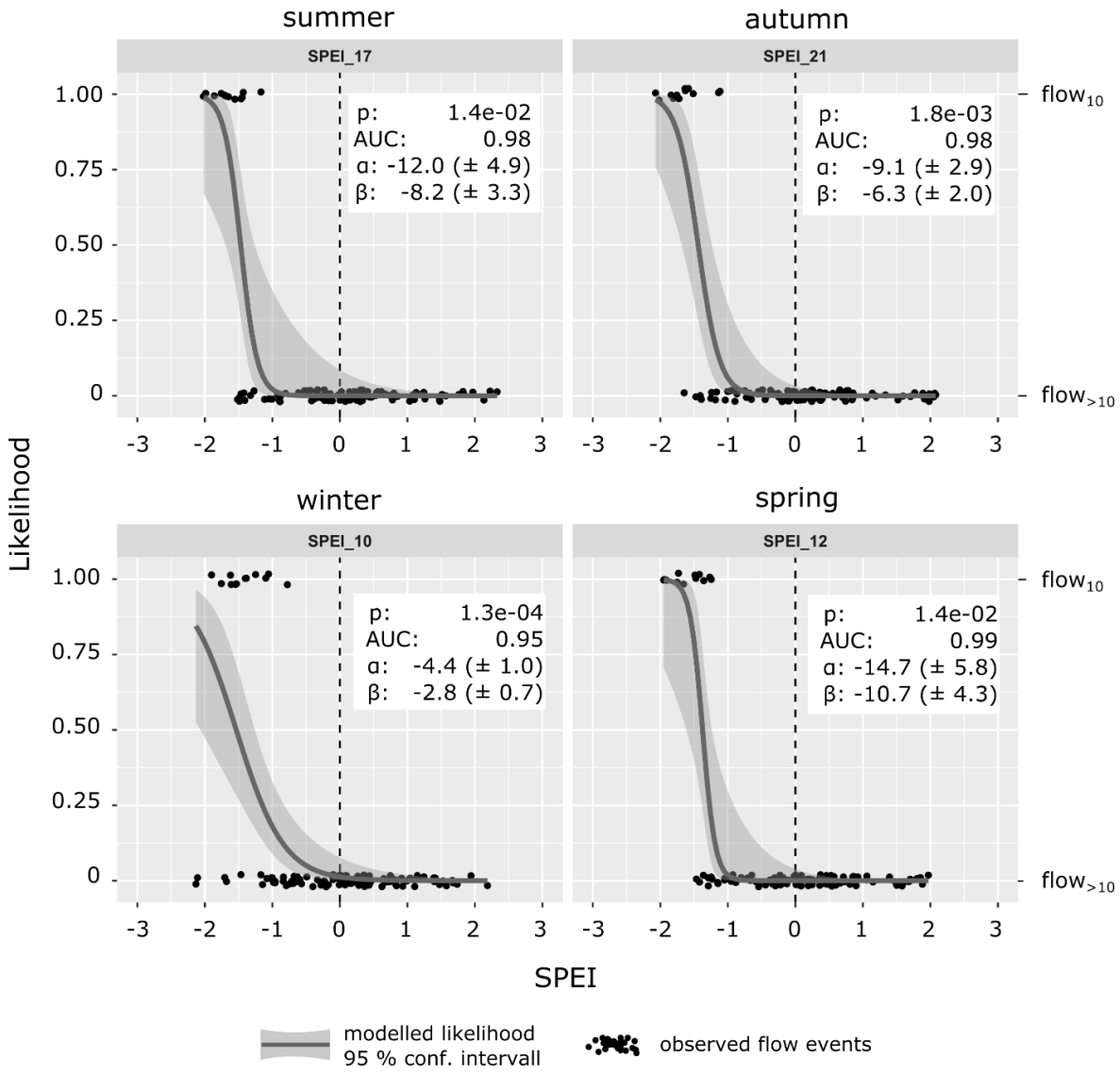

Figure 7: Binary flow model for Murrindindi River (ID 178) in southeast Australia (Melbourne region). α and β = parameter of the logistic regression, AUC = goodness of fit, p = significance level.

Figure 7 shows the seasonal models for the Murrindindi River. The following can be seen here: First, the goodness of fit (AUC, white box) varies slightly per season, but is generally "excellent"

throughout the year (winter: 0.95 - spring: 0.99). Second, the model coefficients α and β (white box) vary per season, too.

It can be seen that, in spring, the Murrindindi River is relatively resistant to meteorological droughts of the past 12 months if they are not too severe (no $flow_{10}$ event for SPEI-12 > -1). However, the number of $flow_{10}$ events rises rapidly if the meteorological drought situation becomes more severe (SPEI-12 < -1). For mild drought conditions (-1.5 > SPEI > -1) the likelihood curve in spring describes a steep rise (absolute α_{spring} and β_{spring} highest of all seasons). The first derivative of the spring curve shows a clear peak at SPEI-12 = -1.4. At this point the increase in likelihood is strongest. Under severe drought conditions (SPEI-12 < -2.0) the likelihood of low flow events is close to 100% (0.97 - 0.99). In spring, the Murrindindi River always encountered a $flow_{10}$ event when SPEI-12 dropped below -1.5. From spring to autumn, the resistance of the streamflow to meteorological anomalies decline. Also reliability of the models (lowest in winter, AUC = 0.91) decline.

In winter, the resistance of the Murrindindi River against meteorological drought is lower than in spring (flatter model curve, absolute α_{spring} and β_{spring} lowest of all seasons). The link between the meteorological signal (SPEI) and the binary response variable ($flow_{10}$ events (1/0)) is less pronounced (AUC_{winter} lowest of all seasons, 0.91). Some $flow_{10}$ events occurred already under mild drought conditions (0 ≤ SPEI-10 < -1) but also some $flow_{>10}$ events occurred even under extreme conditions (SPEI-10 < -2.0). The likelihood of $flow_{10}$ events increased slowly within a wide range of SPEI values below which low flow may or may not occur. The first deviation of the winter curve shows a peak at SPEI-10 = -1.5, but this peak the least pronounced of all seasons, the winter derivative is the flattest of all seasons. For the lowest SPEI-10 on record (-2.2) the likelihood does not exceed 86%.

LINEAR TREND ANALYSIS FOR MURRINDINDI RIVER

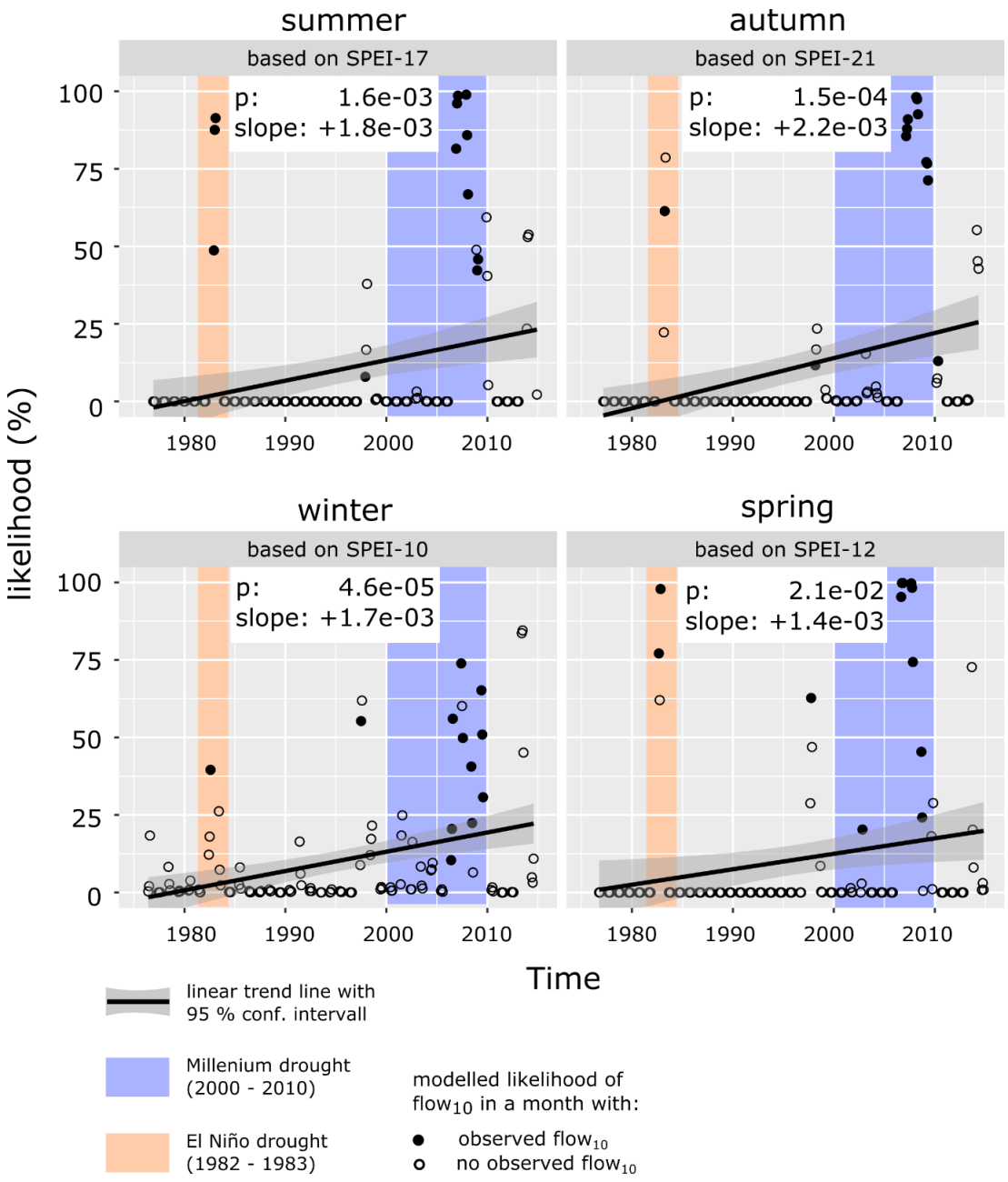

Figure 8: Modelled likelihood of Murrindindi River as a function season specific SPEI time series from January 1975 to December 2014. The likelihood is modeled using Equation 3 with α and β as presented in Figure 7. The solid black line trend line describes the development of the modelled likelihood over time.

Figure 8 displays the modelled likelihood for the Murrindindi River as a function of seasonal specific SPEI time series. It can be seen that likelihood of $flow_{10}$ events significantly increased over all

seasons (positive slope of black trend line). The strongest increase (highest slope of trend line) is observed in autumn ($slope_{autumn}$ = $+2.2e^{-3}$), the weakest increase in spring (slope = $+1.4e^{-3}$). In the second half of the Millennium drought (2005 - 2010) all models show high likelihoods. For example, in autumn, a likelihood between 70% and 100% for the autumn months of the years 2007, 2008 and 2009).

Figure 8 shows furthermore that the modelled likelihood was exceptionally high during the two major drought events in southeast Australia: the Millennium drought (blue) in 2000 - 2010 and the El-Niño drought in 1982-83 (orange).

Also, the hit rates of the models are rather high: a majority of actual $flow_{10}$ events (solid black dots) was recorded for months in which the modelled likelihood is found to be high. In contrast, at months with zero modelled likelihood the Murrindindi River did not encounter any $flow_{10}$ events.

Table 8: Summary statistics of the Murrindindi example

season		summer	autumn	winter	spring
seasonal models	SPEI with highest AUC (acc. period)	17	**21**	10	12
	AUC	0.98	0.98	0.95	**0.99**
	α	-12.0	-9.1	-4.4	**-14.7**
	β	-8.2	-6.3	-2.8	**-10.7**
trend analysis	Significant increase?	YES	**YES**	YES	YES
	slope of trend line	$+1.8e^{-3}$	$\mathbf{+2.2e^{-3}}$	$+1.7e^{-3}$	$+1.4e^{-3}$

4.3.2 All 76 streamflows stations in the Melbourne region

LOGISTIC REGRESSION MODEL

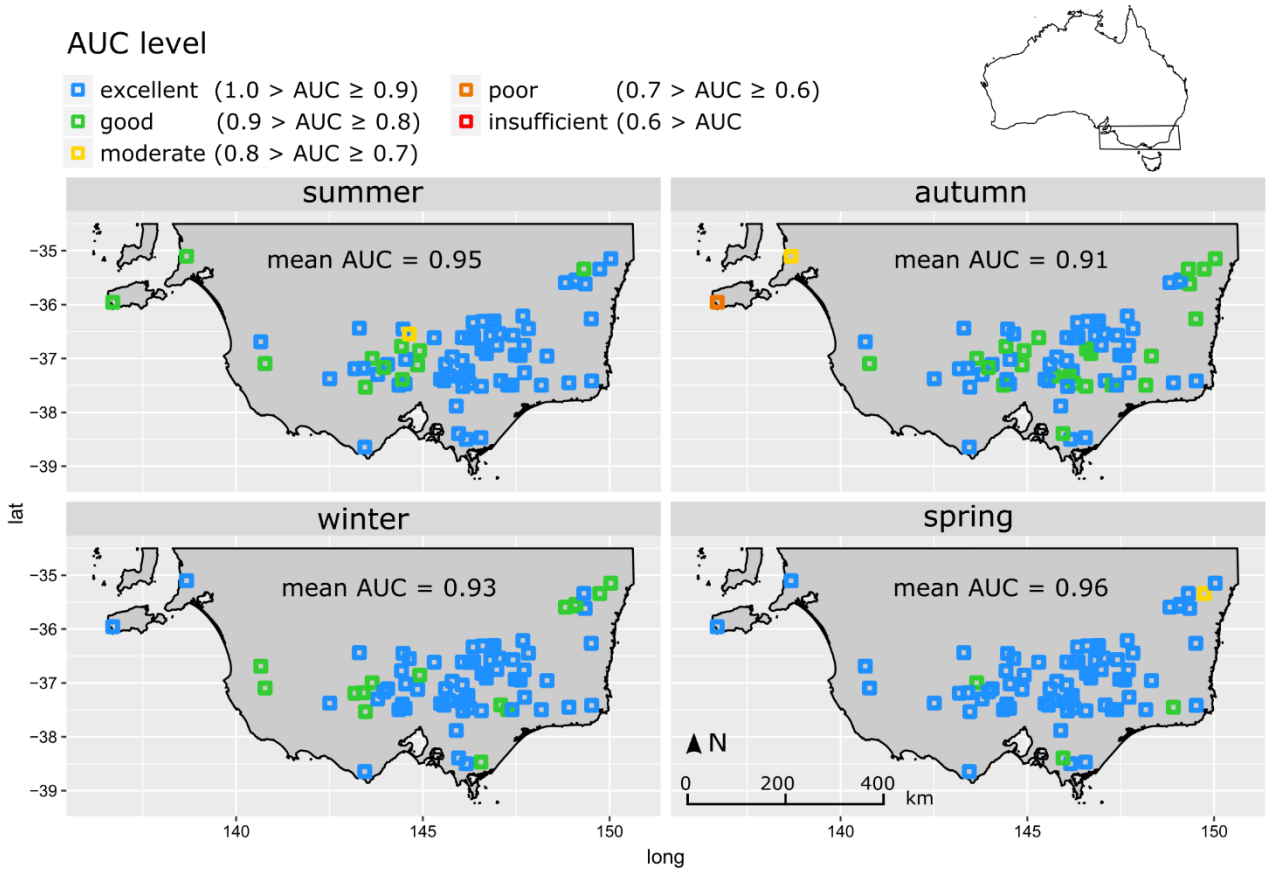

Figure 9: Goodness of fit (AUC) for all 76 stations in the Melbourne region per season. Blue = excellent goodness of fit (1.0 > AUC ≥ 0.9), green = good goodness of fit (0.9 > AUC ≥ 0.8), see top for full classification table.

Figure 9 shows the evolution of AUC values for stations in the Melbourne region throughout the year. It can be seen that the mean goodness of fit is "excellent" over all seasons (≥ 0.9, cf. AUC quality classes in Table 6). The models show the best fit in spring (mean AUC_{spring} = 0.96) with 94% of stations having an "excellent" (≥ 0.9, see classification key, Figure 9 top) and 4% a "good" AUC (0.9 > x ≥ 0.8). High AUC values are reached in summer (mean AUC_{summer} = 0.95) with 84% "excellent" and 14 % "good". From spring to autumn, the mean goodness of fit declines. In autumn (mean AUC_{autumn} = 0.91), 65% of stations show an "excellent" and 32% a "good" AUC. The lowest AUC was observed in autumn (0.69, "poor", ID 12). In total, 38 stations (50%) show "excellent" AUCs over all four seasons, 75 stations (99%) in at least one of the seasons.

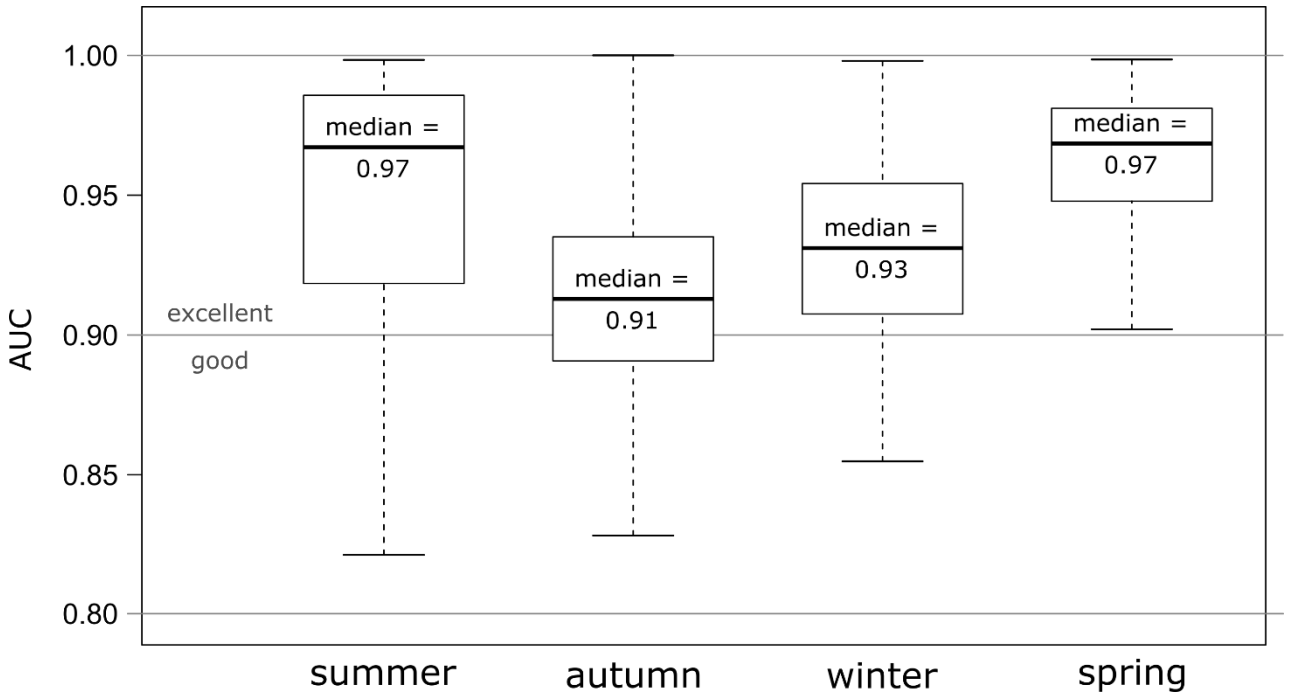

Figure 10: Boxplots of seasonal AUC values for all 76 stations in the Melbourne region. Outliers are not shown.

Figure 10 provides a deeper insight in the evolution of the seasonal AUC values in the Melbourne region, already presented in Figure 9. It can be seen again that the goodness of fit of the models varies throughout the year. The goodness of fit is lowest in autumn. The interquartile range in autumn ranges from 0.89 to 0.93 and is the only one extending below 0.90 ("excellent"). The AUC values in spring and summer are comparably high, however, the variation in spring is distinctly lower than in summer. The link between the meteorological signal (SPEI) and the occurrence of $flow_{10}$ events is strongest in spring. In summer, the link is weaker than in spring for some stations. In autumn, the link is relatively weak for a majority of stations before rising again in winter.

LINEAR TREND ANALYSIS

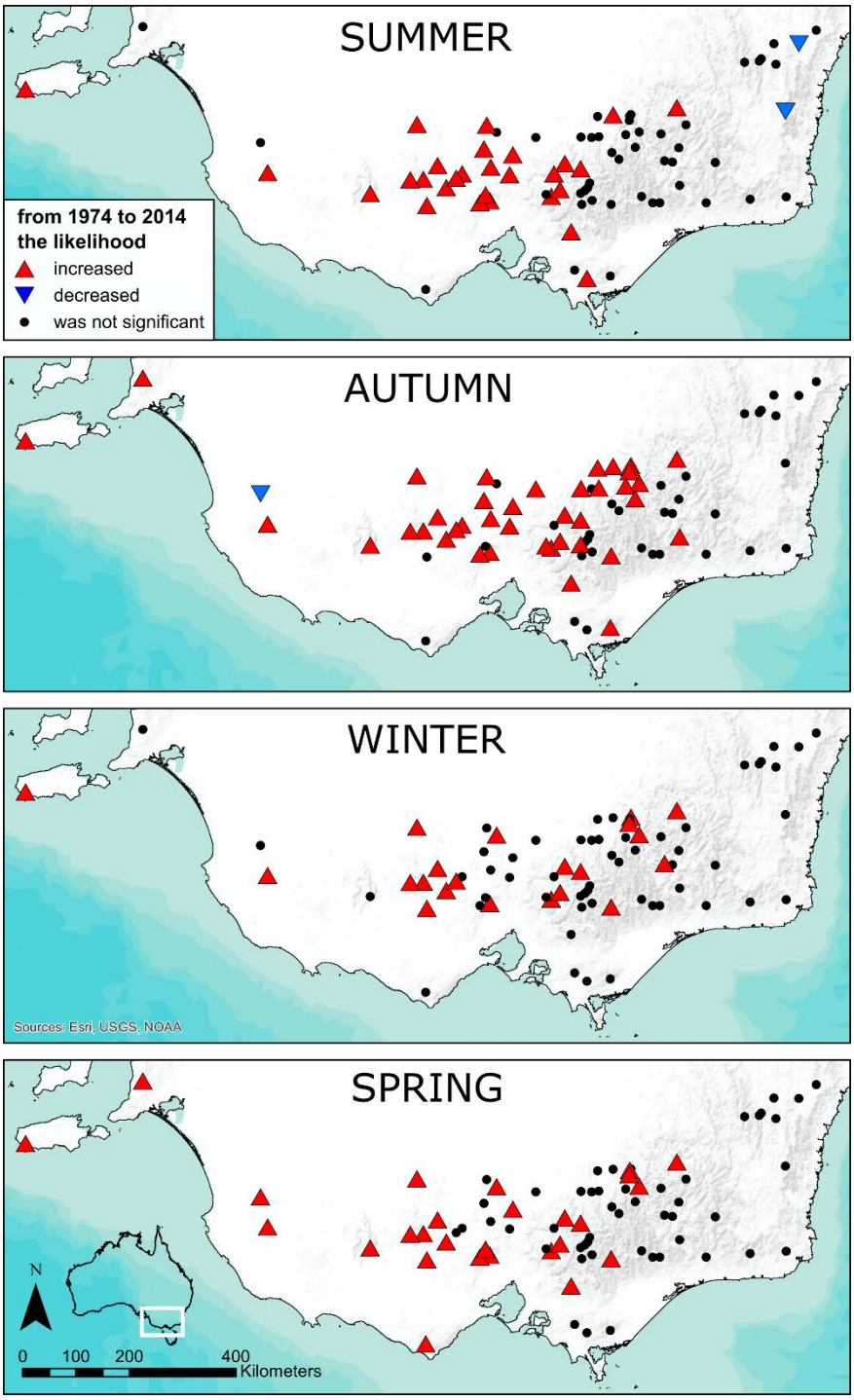

Map 9: Spatial distribution of the $flow_{10}$ likelihood trends, for stations of the Melbourne region, per season. This map shows where the modelled $flow_{10}$ likelihood for the years 1973 to 2014 increased (red), decreased (blue) and where the linear trend line was not significant (white).

Map 9 shows how the seasonal likelihood of $flow_{10}$ events developed between 1973 and 2014. It can be seen that likelihood significantly increased (red) for a large number of stations in the Melbourne region. This increase can be observed throughout the whole year (min: 21 stations in winter, max: 40 stations in autumn). 13 stations (17%) show an increased likelihood over all four seasons, 48 stations (63%) show an increase in at least one season of the year, 33 stations (43%) in at least two seasons.

In contrast, a decreasing likelihood (blue diamonds, Map 9) is observed for 3 stations: 2 in summer (2.6%) and 1 in autumn (1.3%). Among the stations where the trend was not significant (black circles) a large number show a positive trend, only few a negative. A summary of the seasonal trends can be found in Figure 11.

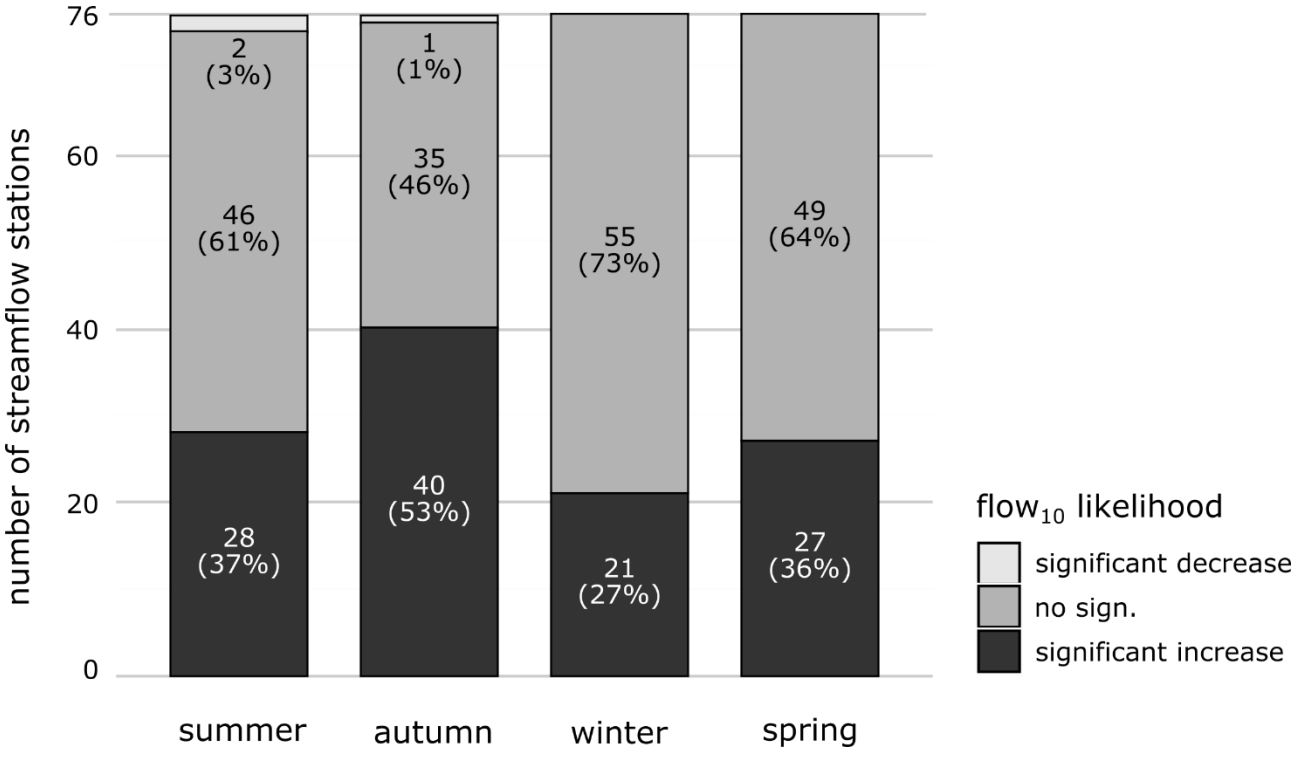

Figure 11: Summary of the seasonal trend analysis. Number and percentage of stations at which the likelihood significantly increased (red), significantly decreased (blue) or no significant change in likelihood was detected (grey).

Table 9: Basic statistics for binary models and the linear trend analysis for the 76 stations in the Melbourne region. (1) Mean, median and sd of accumulation periods that provided the highest AUC und were thus used for modelling. (2) Mean and sd of AUC values that were reached with these SPEI time series. (3) Basic statistics for α and β. (4) Overview on the results of the linear trend analysis of the modelled likelihood over time.

	Season	summer	autumn	winter	spring
Binary models	Mean acc. period of SPEI	10.0	**12.3**	7.2	7.3
	Median acc. period of SPEI	**10.5**	9.5	6.0	6.0
	sd acc. period of SPEI	5.8	**8.4**	5.1	5.0
	Mean AUC	0.95	0.91	0.93	**0.96**
	sd AUC	0.05	0.05	0.04	0.04
trend analysis	Stations with increasing trend	28	**40**	21	27
	Stations with decreasing trend	**2**	1	0	0
	Stations with no sign.	46	35	**55**	49
	Mean slope of linear trend line (stations with significantly positive trend)	$1.8\ e^{-3}$	$\mathbf{2.0\ e^{-3}}$	$1.6e^{-3}$	$1.6e^{-3}$

Table 9 presents an overview of the results presented in this chapter. In spring, short to medium accumulation periods (SPEI-6 to SPEI-8) provide a high goodness of fit. From summer to autumn, the AUC declines while the SPEI times scale increase. The most streamflows with an increase are detected in autumn (n = 40). The least in winter (n = 21).

5 Discussion

5.1 Part I: Are meteorological drought indicators related to streamflow anomalies in Australia?

As expected, the SPEI provided higher correlations than SPI for most parts of the continent, especially in the temperate zones in the south and subtropical zones on the east coast. This superiority of SPEI is in accordance with numerous other studies investigating the correlation between meteorological and hydrological drought indicators (Bachmair et al., 2015; Haslinger et al., 2014; Vicente-Serrano et al., 2014). The superiority of SPEI over SPI reinforces previous findings that temperature and evapotranspiration have a strong effect on streamflows in Australia, as postulated by Cai et al. (2009) and Yu et al. (2010). This accounts especially for the southeastern part of the continent where the superiority of SPEI was most pronounced. Although the absolute mean temperature is higher in the north and although the north encounters a 6 to 9 months long dry period, the SPI provided similarly high or even higher correlations there. This shows that the question if the SPI or the SPEI is better suited to describe streamflow patterns cannot be answered by simply looking at temperature values. Instead, the crucial aspect is the relation between evapotranspiration rates and precipitation and its development throughout the year. This relation is described in the water balance equation. Where the water balances is dominated by precipitation, SPI tends to be stronger, and vice versa, SPEI tends to be stronger where it is dominated by the potential evapotranspiration.

TREND FROM SOUTHEAST TO NORTHWEST

The results presented in the Map 5, Map 6, Map 7 and Map 8 suggest that the responses of rivers to the meteorological signal follow a continental trend. This trend, from southeast to northwest, was evident in: (a) in the relative performance of SPI/SPEI (Map 6), (b) the maximum correlation strength with SSI (Map 7) and (c) the response times on the continent (Map 8).

Generally speaking, a high variability of precipitation throughout the year (as in the northwest) matches with low all-year correlations of SPI/SPEI, a higher response time and a strong performance of SPI in the data set. Vice versa, a low annual variability in rainfall (as in the southeast) coincides

with high correlations, short response times and a superiority of SPEI. These findings are in line with Barker et al. (2016) who postulated a strong relation between rainfall patterns and indicator performances for streamflows in the UK. Additionally to rainfall, Barker et al. (2016) identified a distinct influence of catchment storage and geology on response times.

A CONTINENTAL PRECIPITATION SHIFT AS MAIN INFLUENCING FACTOR?

For Australia, this trend coincides with the overall shift in the precipitation pattern, as presented in Annex 1 with the northwest becoming wetter and southeast becoming drier. That suggests that the hydro-meteorological variability in Australia is highly influenced by continental precipitation changes over the last 40 years, as also postulated by Zhang et al. (2016). Though Zhang et al. (2016) analyzed the full range of 222 hydrologic reference stations in Australia and pursued a different objective (identifying regional changes in annual runoff) a large part of the results in Zhang et al. (2016) are consistent with the conclusions made here. For example, the distinct regional patterns:

In both studies, the results of the southeastern and northwestern stations showed little variation. Substantial variations were found for the stations in northern Queensland (Cairns) and the Central Outback. This accordance underlines the validity of the results herein presented. A minor discrepancy occurred regarding the results for region of Perth. In the thesis at hand, response times and all-year correlation strengths of the Perth group (Western Australia) significantly differed from the results of the Melbourne group (Southeast Australia), but were consistent in Zhang et al. (2016). Possibly the lower number of streamflows (higher quality requirements here) could play a role as well as the larger time period (1950 – 2014 in Zhang et al. (2016) vs 1974 – 2014 in the study at hand) and the generally different research methods.

REGIONAL PERFORMANCE DIFFERENCES AT DIFFERENT ACCUMULATION PERIODS

In general, rivers are fed by different water reservoir types with different residence times, i.e. by soil moisture and surface runoff on the short scale and groundwater inflow on the longer scale (Lorenzo-Lacruz et al., 2013; WMO, 2012). Time series of SPI/SPEI accumulated on short time scales fluctuate heavier, meaning that negative and positive values change more frequently (Vicente-Serrano and López-Moreno, 2005). At those short time scales, SPEI was found to be superior to SPI in southeast Australia (Melbourne, Figure 4). This suggests that the streamflows in the Melbourne region are mainly controlled by inflow from water reservoirs with short residence times (soil moisture, surface runoff) and that these reservoirs are strongly influenced by temperature and evapotranspiration. The results shown in Figure 4 suggest the conclusion that rising temperatures lead, i.e., to a declining soil moisture content and negatively affect the streamflows in the region. Similar conclusions were made by Cai et al. (2009) who showed that rising temperatures in southeast Australia have significantly reduced soil moisture contents and, as a consequence, also reduced inflow rates to the rivers. Cai et al. (2009) suggested that the sensitivity of soil moisture content to temperature changes in the MDRB has risen in the recent decades and will likely continue to rise. This increased sensitivity to soil moisture might lead to more extreme drought impacts on the hydrosphere in the future. This sensitivity is one major concern for the future handling of extreme droughts in southeast Australia and was probably a key reason for the heavy impact of the Millennium drought in the MDRB (Cai et al., 2009).

In contrast, time series of SPI/SPEI accumulated on longer time scales fluctuate less, meaning that the individual dry and wet periods are longer and change less often. At those longer time scales, the SPI performed better than SPEI in the tropical to equatorial northwest (Darwin, Figure 5). This shows that in the precipitation dominated northern climates with heavy monsoons, SPI is the better indicator at any time scale. Although the absolute temperatures are higher in the northwest, SPEI is inferior to SPI because the streamflows are generally controlled by slowly reacting water reservoirs (groundwater) and not by soil moisture or surface runoff. Those groundwater reservoirs are filled during the heavy monsoons in the wet period in late summer and determine the streamflows throughout the rest of the year. The SPI is better capable of representing such hydrologic conditions.

THE NEED FOR SEASON SPECIFIC ANALYSIS

The good performance of SPEI throughout the year in southeast Australia (Figure 6) showed that high all-year correlations do not necessarily originate from high correlations during the high flow season (winter) only. In this case, they were a result of persistently strong connection between the meteorological and the hydrological signal over all seasons. This strengthens the conclusion that the streamflows in this region are influenced by both temperature (in summer) and rainfall (in winter), as suggest by others (Yu et al., 2010; Cai et al., 2009; Cai and Cowan, 2008b).

Furthermore, it highlights the strong impact of rising temperatures and evapotranspiration rates on the streamflows in the Murray-Darling River Basin in summer, also postulated by van Dijk et al. (2013) and Cai and Cowan (2008b). What do these conclusions imply for the choice of the research method? First of all, it shows that the SPEI is capable of describing streamflow patterns both during precipitation dominated wet seasons and during temperature dominated dry seasons. In consequence, an all-year correlation analysis with SPEI can be a valid method when assessing the link between the meteorological and hydrological signal, especially in temperate climate zones with constant rainfalls throughout the year. However, the fact response times varied heavily, both seasonally and regionally, highlights the importance of assessing the correlation strength using various accumulation periods of SPEI, specific to seasons, as already suggested by López-Moreno et al. (2013).

INFLUENCING FACTORS ON REGIONAL RESPONSE TIMES

The high seasonal and regional variations in response times (Figure 6) are well in line with López-Moreno et al. (2013). The authors of this study outlined several mechanisms that could explain the development of different response times in a semi-arid mountain basin. They showed that response times in the Ebro basin northern Spain were influenced by an interaction of geology, groundwater storages, accumulated snow packs and dam operations.

These findings may be partly transferred to southeast Australia as the region is similar to the Ebro basin in Spain. Following the findings of López-Moreno et al. (2013), the results presented in Figure 6 might be explained as following: In winter, large rainfalls lead to a high runoff and homogenously short response times in the whole region. In spring, decreasing rainfalls and rising temperatures favor longer accumulation periods of SPEI. Additionally, snow melting processes in some parts of

the mountain ranges lead to a delay of the meteorological signal at some stations and thus to a higher regional variation. In summer and autumn, the high variation in response times might be a result of a generally low runoff and a stronger influence of different infiltration characteristics related to the highly diverse geology in the region.

Furthermore, the development of different response times in Southeast Australia might also be related to regional water management strategies. Media reports of 2011 revealed that the Murrumbidgee River suffered from unmonitored damming activities in its upper reaches (SMH, 2011). Accordingly, this river showed strongly fluctuating response times from one month in autumn to nine months in spring. This and the high number of dams in Victoria (450,000 according to DEPI 2014) suggest that water management activities have an influence on the results, especially in summer and autumn when the water extraction rates from the local rivers for irrigation purpose are highest. Such a link was also suggested by Vicente-Serrano and López-Moreno (2005).

However, reliable data on water release rates and damming activities is needed to pin this down, but was not available for the region.

5.2 Part II: Are meteorological drought indicators related to the occurrence of low flow in southeast Australia?

In part two of the thesis, the explanatory power of SPEI to predict low flow events was assessed using seasonal binary models. The models were applied on the best fitting SPEI time series and a linear trend analysis was conducted to evaluate how the likelihood to observe a $flow_{10}$ event developed over time.

The results showed that:

1) Seasonally adjusted time series of SPEI have a high potential of realistically quantifying the likelihood of low flow events in southeast Australia.
2) Between 1974 and 2014, the likelihood of low flow increased at a large number of streamflow stations in the region. The increase is strongest in autumn. However, also the goodness of fit of the logisitic regression model was found to be lowest in autumn (Figure 9 and Figure 10). The strongest link between the SPEI and $flow_{10}$ events was found in spring.

The crucial factor for the development of hydrological droughts in southeast Australia is the wetting period in late autumn and winter. This is suggested by evolution of the seasonal AUC values. Spring marks the end of this wetting period. The fact that accumulation of seven months provided the highest goodness of fit for spring implies that the occurrence of low flow in spring is closely linked to the rainfalls in winter and autumn. The strength of this link declines from spring to autumn before rising again in winter. This shows that the influence of the winter rainfalls declines the further into the dry period, however they remain a key factor throughout the year.

The models show that the closer to these wetting period the more sensitive the reaction of the rivers to the meteorological anomalies. In spring, the rivers in southeast Australia were found to relatively resistant to mild meteorological droughts (SPEI-7 < -1). However the system quickly collapses when the SPEI-7 drops below a critical value. This sensitivity to the meteorological drought situation declines from spring to autumn. One reason for that could be lower fluctuations in spring and summer rainfalls in comparison to winter rainfalls or just the fact that rainfalls in winter are stronger than in summer.

THE "SPECIAL ROLE OF AUTUMN" IN SOUTHEAST

One key finding of this thesis is that autumn results differed in many ways from the results in other seasons. One reason for this difference could be, as mentioned above, that the streamflows are mainly influenced by abundant rainfalls in winter. The further into the dry season the smaller the influence of these winter rainfalls and the higher the uncertainties.

However, there are also indices suggesting that the high uncertainties in autumn might be related to a general change in autumn climate in the region. The "special role of autumn" in the southeast and its importance in the development of hydrological anomalies has also been investigated by others (van Dijk et al., 2013; Verdon-Kidd and Kiem, 2009; Cai and Cowan, 2008a) with sometimes contrasting results.

Cai and Cowan (2008b) showed that the annual inflow rates in the southern Murray-Darling River Basin are most sensitive to rainfall fluctuations in autumn. This is worth mentioning because one key factor for the development of the Millennium drought were strong rainfall reductions in this seasons (van Dijk et al., 2013; Verdon-Kidd and Kiem, 2009; Cai and Cowan, 2008a). Figure 8 suggest that mainly responsible for the significant increase of likelihood at Murrindindi River were high likelihoods during the Millennium drought. This could explain why in autumn the mean increase of likelihood was found to be higher than in any other season. It could also explain the general tendency of a stronger drought impact in autumn as shown in Map 9.

Are the observed uncertainties in autumn a result of a greater climate change induced shift in the region, as proposed by Chiew et al. (2011) and Cai and Cowan (2008a)? Further analysis could bring valuable information here.

Zhang et al. (2016) analyzed similar data set using a different approach. A comparison between both studies revealed, as expected, commonalities and discrepancies. In line with this thesis, Zhang et al. (2016) detected evidence for runoff reductions over all seasons. Also, autumn was found to be an extraordinary season (i.e. the only seasons in which no station showed an increase in runoff anywhere in Australia).

Another commonality between both studies is the finding that autumn was the season loaded with the highest uncertainties. In this thesis, the average seasonal AUC was lowest in autumn (AUC_{autumn} = 0.91, Figure 9) meaning that the autumn specific SPEI time series were least capable of

serving as a predictor of $flow_{10}$ events. Zhang et al. (2016) found that – after testing the runoff time series for randomness – a large number of autumn time series (44% of 222 stations) were biased - predominantly in the Murray-Darling River basin. Additionally, the number of biased time series where exceptionally high during low flow (q10, 75% of 222 stations). A detailed bias analysis could bring further information here.

WHAT ELSE MAY INFLUENCE THE OCCURRENCE OF LOW FLOW EVENTS?

The seasonal and regional fluctuations in the AUC values (Figure 9) suggest that changes in the likelihood of low flow events may not only be influenced by precipitation and temperature. Besides the ones discussed above many other factors may contribute to increased likelihoods for low flow. In the past, anthropogenic factors (river damming, irrigation and land use) have certainly favored the development of hydrological droughts in the Murray-Darling River basin. Also, ecological factors (soil degradation, erosion, increased hydrophobicity after long dry periods) may play a role here and should be considered when interpreting the results of this thesis. Also, natural catchment characteristics (topography, slope, geology) were not included in the analysis and might have different consequences for the occurrence of low flow events, too. Last but not least, the Australian climate is a highly variable by nature due to the size and geographical position of the continent and the complexity of its driving mechanisms.

All these aspects make it difficult to detect significant trends in likelihood time series. Also, assigning identified trends to a precise cause is challenging, as temperature, precipitation and streamflow data underlie high natural fluctuations that may or may not be subject to a general change in climate or drought characteristics. That shows that a good understanding of the region is important when interpreting likelihood trends based on meteorological predictors. It also highlights the necessity to carefully analyze model outputs for each streamflow station separately before making conclusions on a wider regional or continental scale.

5.3 Part II: Are meteorological drought indicators related to the occurrence of low flow at the Murrindindi River?

The Murrindindi River was chosen as a sample station to deeper explore the capability of SPEI to predict low flow events.

As shown in Figure 8, the SPEI based model is capable of accurately carving out major drought events in retrospect. For the drought years 1982/83 (El Niño drought) and the 2000 to 2010 (Millennium drought) the seasonal models provided distinctly increased likelihoods across all seasons. Those high likelihood matched very well with the occurrence of actually observed $flow_{10}$ events (high "hit rate"). Vice versa, the modelled likelihood was close to zero during non-drought years and matched very well with the occurrence of $flow_{>10}$ events (low "false alarm rate").

These findings imply the following conclusion:

(1) The hydrological drought situation at the Murrindindi River is strongly linked to the meteorological drought situation of longer times scale (12 to 21 months). The high seasonal accuracy of the SPEI based models (Figure 9) is an indication for the strong impact of temperature and increased evapotranspiration rates on the streamflows in the region, as already postulated for Australia (Yu et al., 2010; Cai et al., 2009; Cai and Cowan, 2008b; Nicholls, 2004) and for other semi-arid regions of the world (Vicente-Serrano et al., 2014 and Teuling et al., 2013).

The high AUCs values for longer time scales of SPEI (12 to 21 months) indicate that there is a steady inflow to the Murrindindi from water sources with longer residence times. These water sources prevent the Murrindindi from falling dry under mild drought conditions. However, when the drought situation exacerbates, the likelihood of low flow increases rapidly. The strength of this increase and the consequences for the river vary across the year. The steepness of the spring curve suggest the existence of a sharp SPEI threshold (SPEI-12 = -1.4) below which the water supply for Murrindindi quickly collapses. The sensitivity of the streamflow towards this threshold is very high (likelihood curve close to 100%, no $flow_{>10}$ events on record below threshold).

In winter, the link between the meteorological signal and the occurrence of $flow_{10}$ events was found to be less pronounced (AUC 0.95). The best fitting SPEI time series (SPEI-21) was not capable of providing a sharp threshold below which the likelihood of low flow would occur. Instead $flow_{10}$ events happened within a range of SPEI values.

In the spring months from 1974 to 2014, no $flow_{10}$ events were recorded when the SPEI-12 was greater than -1. This suggests that water sources generated over the past 12 months provided a steady water supply to the Murrindindi River. Those sources were large enough to compensate inflow deficits on a shorter scales. However, they are prone to entirely collapsing under more severe drought conditions.

5.4 Influence of autocorrelation

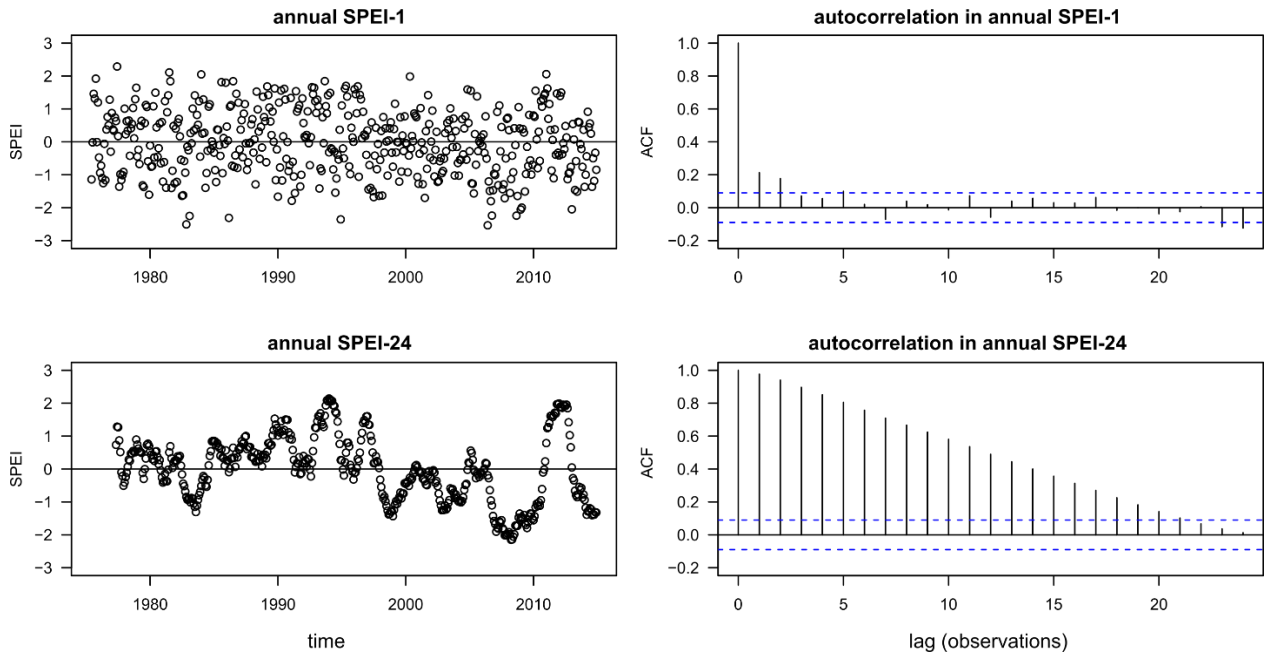

Figure 12: Annual autocorrelation in SPEI time series at station 178 (Murrindindi River), top: SPEI-1, bottom: SPEI-24. Left side: development of annual SPEI over time Right side: autocorrelation plot with significance line (blue).

Figure 12 shows the autocorrelation analysis for annual time series of SPEI-1 and SPEI-24 at the Murrindindi River (ID 178). It can be seen that the time series are autocorrelated to a certain degree. Generally, autocorrelations in the data set increased with growing accumulation periods of SPEI. Long accumulation periods showed a strong autocorrelation up to lags of 15 to 20 observations.

Autocorrelations may lead to a higher risk of type I errors. This might have affected the correlation analysis in part I of the thesis producing artificially high significance levels for longer accumulation periods of SPI/SPEI.

The effect of autocorrelations on the seasonal results (Figure 6) are probably weaker, as shown in the following Figure 13. This figure displays the seasonal autocorrelations in SPEI-1 and SPEI-24 for station 178. Seasonal time series of shorter accumulation periods (SPEI-1 to SPEI-4) still show some seasonality, however for most of the stations in the data set not at a significant level. Time series of longer accumulation periods (SPEI-15 to SPEI-24) showed autocorrelation mainly for lags of 1 to 5 observations.

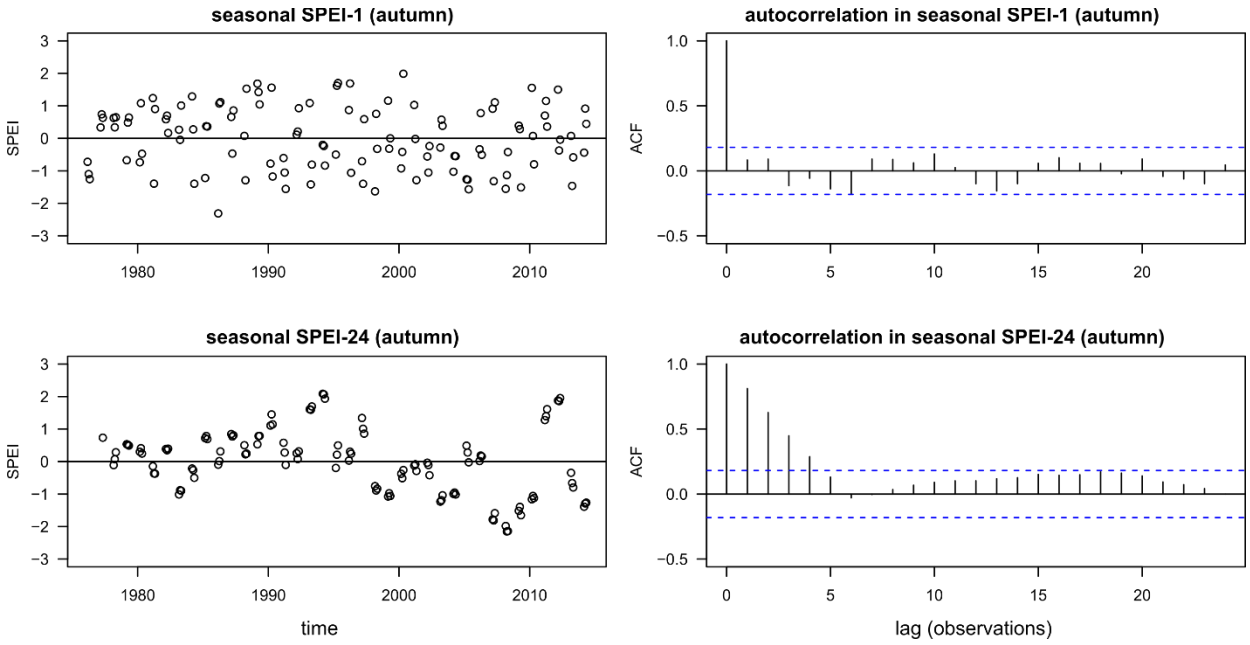

Figure 13: Seasonal autocorrelations (by the example of autumn) in SPEI time series at station 178 (Murrindindi River), top: SPEI-1, bottom: SPEI-24. Left side: development of autumn SPEI over time. Right side: autocorrelation plot with significance line (blue).

One way to reduce the risk of type 1 errors could be adjusting the degrees of freedom during the calculation of the different significance levels (Bachmair et al., 2015). However, the results show that autocorrelation should definitely be considered when using similar approaches in the future.

6 Conclusions

This thesis aimed at assessing the capability of meteorological drought indicators to predict hydrological anomalies in Australia. The analysis was based on long-term runoff, temperature and rainfall records for 152 hydrological reference stations across the Australian continent.

The results may increase the understanding of how streamflows in Australia react to meteorological anomalies in the future. It may also help to improve the Australian drought monitoring and early warning system and provide valuable information for irrigation planning and drought adaptation in Australia.

The key findings and implications are:

- Rising temperatures and increasing evapotranspiration rates have a strong impact on the Australian hydrosphere. This impact is most evident in the southeast where the superiority of SPEI over SPI was most pronounced. Regional variations in response times might be related to the general shift of the continental rainfall patterns in the past decades with the northwest becoming wetter and the southeast becoming drier.
- The link between the meteorological and hydrological signal was found to be strongest in the southeast. The fact that this link remained strong throughout the year highlights the need for the drought research community to intensify efforts towards understanding the regional effects of climate change. As the southeast is home to Australia's most important agricultural region the projected temperature increase may have strong repercussions on irrigation and hydropower capacities. The results from the logistic regression model may increase the understanding of which river in the region may be prone to low flow under a specific meteorological condition. This may provide valuable information to regional stakeholders (such as farmers and fishermen, dam operators and energy companies, environmentalists, local authorities and private persons living in the region) when allocating budgets for water infrastructure and water security projects in the region. It may also help minimizing ecological and economical losses related to streamflow droughts in the basin.
- The results support the assumption that over the last decades the risk of low runoff significantly increased in southeast Australia. A majority of stations (63%) in the greater Melbourne area showed a significantly increased likelihood during at least one season of the

year. Only three stations showed seasonal decrease. Seasonal uncertainties were found to be highest in autumn, possibly an effect of a increased rainfall reduction in autumn.

7 References

ABoS (2008): Water and the Murray-Darling Basin. A Statistical Profile (2000–01 to 2005–06). In *Australian Bureau of Statistics, Canberra,* checked on 4/28/2017.

Bachmair, S.; Kohn, I.; Stahl, K. (2015): Exploring the link between drought indicators and impacts. In *Nat. Hazards Earth Syst. Sci.* 15 (6), pp. 1381–1397. DOI: 10.5194/nhess-15-1381-2015.

Bachmair, Sophie; Stahl, Kerstin; Collins, Kevin; Hannaford, Jamie; Acreman, Mike; Svoboda, Mark et al. (2016): Drought indicators revisited. The need for a wider consideration of environment and society. In *WIREs Water* 3 (4), pp. 516–536. DOI: 10.1002/wat2.1154.

Barker, Lucy J.; Hannaford, Jamie; Chiverton, Andrew; Svensson, Cecilia (2016): From meteorological to hydrological drought using standardised indicators. In *Hydrol. Earth Syst. Sci.* 20 (6), pp. 2483–2505. DOI: 10.5194/hess-20-2483-2016.

Blauhut, Veit; Gudmundsson, Lukas; Stahl, Kerstin (2015): Towards pan-European drought risk maps. Quantifying the link between drought indices and reported drought impacts. In *Environ. Res. Lett.* 10 (1), p. 14008. DOI: 10.1088/1748-9326/10/1/014008.

Blauhut, Veit; Stahl, Kerstin; Stagge, James Howard; Tallaksen, Lena M.; Stefano, Lucia de; Vogt, Jürgen (2016): Estimating drought risk across Europe from reported drought impacts, drought indices, and vulnerability factors. In *Hydrol. Earth Syst. Sci.* 20 (7), pp. 2779–2800. DOI: 10.5194/hess-20-2779-2016.

BoMA (2017a): Australian Climate Influences. Bureau of Meteorology Australia. Melbourne. Available online at www.bom.gov.au/climate/about, checked on 5/2/2017.

BoMA (2017b): Climate Data Online. Bureau of Meteorology Australia. Melbourne. Available online at http://www.bom.gov.au/climate/data/, checked on 3/21/2017.

BoMA (2017c): Streamflow data quality codes for Hydrologic Reference Stations. Bureau of Meteorology Australia. Melbourne. Available online at http://www.bom.gov.au/water/hrs/qc_doc.shtml, checked on 2/23/2017.

BoMA (2017d): What are La Niña/El Niño and how does it impact Australia? Bureau of Meteorology Australia. Available online at http://www.bom.gov.au/climate/updates/articles/a020.shtml, checked on 4/25/2017.

Cai, Wenju; Cowan, Tim (2008a): Dynamics of late autumn rainfall reduction over southeastern Australia. In *Geophys. Res. Lett.* 35 (9), L02606. DOI: 10.1029/2008GL033727.

Cai, Wenju; Cowan, Tim (2008b): Evidence of impacts from rising temperature on inflows to the Murray-Darling Basin. In *Geophys. Res. Lett.* 35 (7), n/a-n/a. DOI: 10.1029/2008GL033390.

Cai, Wenju; Cowan, Tim; Briggs, Peter; Raupach, Michael (2009): Rising temperature depletes soil moisture and exacerbates severe drought conditions across southeast Australia. In *Geophys. Res. Lett.* 36 (21). DOI: 10.1029/2009GL040334.

Chiew, F. H. S.; McMahon, T. A. (1993): Detection of trend or change in annual flow of Australian rivers. In *Int. J. Climatol.* 13 (6), pp. 643–653. DOI: 10.1002/joc.3370130605.

Chiew, F. H. S.; Piechota, T. C.; Dracup, J. A.; McMahon, T. A. (1998): El Nino/Southern Oscillation and Australian rainfall, streamflow and drought: Links and potential for forecasting. In *Journal of Hydrology* 204 (1), pp. 138–149.

Chiew, F. H. S.; Young, W. J.; Cai, W.; Teng, J. (2011): Current drought and future hydroclimate projections in southeast Australia and implications for water resources management. In *Stoch Environ Res Risk Assess* 25 (4), pp. 601–612. DOI: 10.1007/s00477-010-0424-x.

Chou, Yue Hong; Minnich, Richard A.; Chase, Richard A. (1993): Mapping probability of fire occurrence in San Jacinto Mountains, California, USA. In *Environmental Management* 17 (1), pp. 129–140. DOI: 10.1007/BF02393801.

Collins, Kevin; Hannaford, Jamie; Svoboda, Mark; Knutson, Cody; Wall, Nicole; Bernadt, Tonya et al. (2016): Stakeholder Coinquiries on Drought Impacts, Monitoring, and Early Warning Systems. In *Bull. Amer. Meteor. Soc.* 97 (11), ES217-ES220. DOI: 10.1175/BAMS-D-16-0185.1.

CSIRO (2015): Climate change in Australia | Regional Report. In *Commonwealth Scientific and Industrial Research Organisation. DOI:* 10.1515/9781400879533-005.

Dai, Aiguo (2011): Drought under global warming. A review. In *WIREs Clim Change* 2 (1), pp. 45–65. DOI: 10.1002/wcc.81.

Deo, Ravinesh C.; Byun, Hi-Ryong; Adamowski, Jan F.; Begum, Khaleda (2016): Application of effective drought index for quantification of meteorological drought events. A case study in Australia. In *Theor Appl Climatol. DOI:* 10.1007/s00704-015-1706-5.

DEPI (2014): Dams in Victoria. Edited by Department of Environment, Land, Water and Planning, Victoria. Available online at http://www.depi.vic.gov.au/water/governing-water-resources/dams, updated on 3/24/2017, checked on 4/3/2017.

Economist (Ed.) (2007): Australia's costly drought. Newspaper Limited. Available online at http://www.economist.com/node/9065059, checked on 12/2/2016.

Eilertz, Daniel Robert (2013): The linkage between meteorological drought indicators and streamflow patterns across Europe. Master thesis. Albert-Ludwig-Universität, Freiburg. Institute of Hydrology.

Gudmundsson, L.; Rego, F. C.; Rocha, M.; Seneviratne, S. I. (2014): Predicting above normal wildfire activity in southern Europe as a function of meteorological drought. In *Environ. Res. Lett.* 9 (8), p. 84008. DOI: 10.1088/1748-9326/9/8/084008.

Gudmundsson, L.; Stagge, James H. (2016): SCI: Standardized Climate Indices such as SPI, SRI or SPEI. R package desciption 1.0-2. Available online at https://rdrr.io/cran/SCI/man/SCI-package.html, updated on 5/8/2017.

Hannaford, J.; Lloyd-Hughes, B.; Keef, C.; Parry, S.; Prudhomme, C. (2011): Examining the large-scale spatial coherence of European drought using regional indicators of precipitation and streamflow deficit. In *Hydrol. Process.* 25 (7), pp. 1146–1162. DOI: 10.1002/hyp.7725.

Hargreaves, George H. (1994): Defining and Using Reference Evapotranspiration. In *Journal of Irrigation and Drainage Engineering* 120 (6), pp. 1132–1139. DOI: 10.1061/(ASCE)0733-9437(1994)120:6(1132).

Haslinger, Klaus; Koffler, Daniel; Schöner, Wolfgang; Laaha, Gregor (2014): Exploring the link between meteorological drought and streamflow. Effects of climate-catchment interaction. In *Water Resour. Res.* 50 (3), pp. 2468–2487. DOI: 10.1002/2013WR015051.

Hijmans, R.J; van Etten, J.; et al (2016): raster: Geographic Data Analysis and Modeling (r-package description). Available online at https://cran.r-project.org/web/packages/raster/index.html, checked on 5/3/2017.

Kiem, A. S.; Verdon-Kidd, D. C. (2010): Towards understanding hydroclimatic change in Victoria, Australia – preliminary insights into the "Big Dry". In *Hydrol. Earth Syst. Sci.* 14 (3), pp. 433–445. DOI: 10.5194/hess-14-433-2010.

Kiem, Anthony S.; Johnson, Fiona; Westra, Seth; van Dijk, Albert; Evans, Jason P.; O'Donnell, Alison et al. (2016): Natural hazards in Australia. Droughts. In *Climatic Change* 139 (1), pp. 37–54. DOI: 10.1007/s10584-016-1798-7.

Kirono, D.G.C.; Kent, D. M.; Hennessy, K. J.; Mpelasoka, F. (2011): Characteristics of Australian droughts under enhanced greenhouse conditions. Results from 14 global climate models. In *Journal of Arid Environments* 75 (6), pp. 566–575. DOI: 10.1016/j.jaridenv.2010.12.012.

Li, Xing; He, Binbin; Quan, Xingwen; Liao, Zhanmang; Bai, Xiaojing (2015): Use of the Standardized Precipitation Evapotranspiration Index (SPEI) to Characterize the Drying Trend in Southwest China from 1982–2012. In *Remote Sensing* 7 (8), pp. 10917–10937. DOI: 10.3390/rs70810917.

López-Moreno, J. I.; Vicente-Serrano, S. M.; Zabalza, J.; Beguería, S.; Lorenzo-Lacruz, J.; Azorin-Molina, C.; Morán-Tejeda, E. (2013): Hydrological response to climate variability at different time scales. A study in the Ebro basin. In *Journal of Hydrology* 477, pp. 175–188. DOI: 10.1016/j.jhydrol.2012.11.028.

Lorenzo-Lacruz, J.; Vicente-Serrano, S. M.; González-Hidalgo, J. C.; López-Moreno, J. I.; Cortesi, N. (2013): Hydrological drought response to meteorological drought in the Iberian Peninsula. In *Clim. Res.* 58 (2), pp. 117–131. DOI: 10.3354/cr01177.

Mason, J. S.; Graham, N. E. (2002): Areas beneath the relative operating characteristics (ROC) and relative operating levels (ROL) curves: Statistical significance and interpretation. In *Quarterly Journal of the Royal Meteorological Society* 128 (584), 1477-870X.

McFarlane, Don; Stone, Roy; Martens, Sasha; Thomas, Jonathan; Silberstein, Richard; Ali, Riasat; Hodgson, Geoff (2012): Climate change impacts on water yields and demands in south-western Australia. In *Journal of Hydrology* 475, pp. 488–498. DOI: 10.1016/j.jhydrol.2012.05.038.

McKee, T. B.; Doesken, N. J.; Kleist, J. (1993): The relationship of drought frequency and duration to time scales. In *Proceedings of the 8th Conference on Applied Climatology* 1993, pp. 179–183, checked on 2/23/2017.

Mpelasoka, F.; Hennessy, K.; Jones, R.; Bates, B. (2008): Comparison of suitable drought indices for climate change impacts assessment over Australia towards resource management. In *Int. J. Climatol.* 28 (10), pp. 1283–1292. DOI: 10.1002/joc.1649.

Nicholls, Neville (2004): The Changing Nature of Australian Droughts. In *Climatic Change* 63 (3), pp. 323–336. DOI: 10.1023/B:CLIM.0000018515.46344.6d.

Palmer, Wayne C. (1965): Meteorological Drought. In *Research Paper No. 45*.

Peel, M. C.; Finlayson, B. L.; McMahon, T. A. (2007): Updated world map of the Köppen-Geiger climate classification. In *Hydrol. Earth Syst. Sci. Discuss.* 4 (2), pp. 439–473. DOI: 10.5194/hessd-4-439-2007.

Peterson, W. W.; Birdsall, T. G. (1953): The theory of signal detectability : Part I, the general theory : Part II, applications with Gaussian noise. University of Michigan. Ann Arbor. In *College of Engineering. Technical Reports,* checked on 2/24/2017.

Potter, N. J.; Chiew, F. H. S. (2011): An investigation into changes in climate characteristics causing the recent very low runoff in the southern Murray-Darling Basin using rainfall-runoff models. In *Water Resour. Res.* 47 (12), n/a-n/a. DOI: 10.1029/2010WR010333.

Potter, N. J.; Chiew, F.H.S.; Frost, A. J. (2010): An assessment of the severity of recent reductions in rainfall and runoff in the Murray–Darling Basin. In *Journal of Hydrology* 381 (1-2), pp. 52–64. DOI: 10.1016/j.jhydrol.2009.11.025.

Rahmat, Siti Nazahiyah; Jayasuriya, Niranjali; Bhuiyan, Muhammed (2015): Assessing droughts using meteorological drought indices in Victoria, Australia. In *Hydrology Research* 46 (3), p. 463. DOI: 10.2166/nh.2014.105.

Reisinger, A.; Kitching, R. L.; Chiew, F.; Hughes, L.; Newton, P. C. D.; Schuster, S. S. et al. (2014): Australasia. In V. R. Barros, C. B. Field, D. J. Dokken, M. D. Mastrandrea, K. J. Mach, T. E. Bilir et al. (Eds.): Climate Change 2014: Impacts, Adaptation, and Vulnerability. Part B: Regional Aspects. Contribution of Working Group II to the Fifth Assessment Report of the Intergovernmental Panel of Climate Change. Cambridge, United Kingdom and New York, NY, USA: Cambridge University Press, pp. 1371–1438.

Saft, Margarita; Peel, Murray C.; Western, Andrew W.; Zhang, Lu (2016): Predicting shifts in rainfall-runoff partitioning during multiyear drought. Roles of dry period and catchment characteristics. In *Water Resour. Res. DOI:* 10.1002/2016WR019525.

SMH (2011): Murrumbidgee starved because of man-made drought. With assistance of Debra Jopson. Sydney Morning Herald Newspaper. Available online at http://www.smh.com.au/environment/water-issues/murrumbidgee-starved-because-of-manmade-drought--report-20110207-1ak9n.html, checked on 3/31/2017.

Stagge, James H.; Tallaksen, Lena M.; Gudmundsson, Lukas; van Loon, Anne F.; Stahl, Kerstin (2015): Candidate Distributions for Climatological Drought Indices (SPI and SPEI). In *Int. J. Climatol.* 35 (13), pp. 4027–4040. DOI: 10.1002/joc.4267.

Stone, Roger C. (2014): Constructing a framework for national drought policy. The way forward – The way Australia developed and implemented the national drought policy. In *Weather and Climate Extremes* 3, pp. 117–125. DOI: 10.1016/j.wace.2014.02.001.

Teuling, Adriaan J.; van Loon, Anne F.; Seneviratne, Sonia I.; Lehner, Irene; Aubinet, Marc; Heinesch, Bernard et al. (2013): Evapotranspiration amplifies European summer drought. In *Geophys. Res. Lett.* 40 (10), pp. 2071–2075. DOI: 10.1002/grl.50495.

Tijdeman, E.; van Loon, A. F.; Wanders, Niko; van Lanen, H. A. J. (2012): The effect of climate on droughts and their propagation in different parts of the hydrological cycle. In *Tech. Rept. EU Drought R&SPI project* (2), pp. 1–70. Available online at http://www.eu-drought.org/media/default.aspx/emma/org/10814118/DROUGHT-RSPI+Technical+Report+No.+2+-+The+effect+of+climate+on+droughts+and+their+propagation+in+different+parts+of+the+hydrological+cycle.pdf, checked on 3/3/2017.

van Dijk, Albert I. J. M.; Beck, Hylke E.; Crosbie, Russell S.; Jeu, Richard A. M. de; Liu, Yi Y.; Podger, Geoff M. et al. (2013): The Millennium Drought in southeast Australia (2001-2009). Natural and human causes and implications for water resources, ecosystems, economy, and society. In *Water Resour. Res.* 49 (2), pp. 1040–1057. DOI: 10.1002/wrcr.20123.

van Lanen, Henny A.J.; Laaha, Gregor; Kingston, Daniel G.; Gauster, Tobias; Ionita, Monica; Vidal, Jean-Philippe et al. (2016): Hydrology needed to manage droughts. The 2015 European case. In *Hydrol. Process.* 30 (17), pp. 3097–3104. DOI: 10.1002/hyp.10838.

van Loon, Anne F.; Stahl, Kerstin; Di Baldassarre, Giuliano; Clark, Julian; Rangecroft, Sally; Wanders, Niko et al. (2016): Drought in a human-modified world. Reframing drought definitions, understanding, and analysis approaches. In *Hydrol. Earth Syst. Sci.* 20 (9), pp. 3631–3650. DOI: 10.5194/hess-20-3631-2016.

Verdon-Kidd, Danielle C.; Kiem, Anthony S. (2009): Nature and causes of protracted droughts in southeast Australia. Comparison between the Federation, WWII, and Big Dry droughts. In *Geophys. Res. Lett.* 36 (22), p. 138. DOI: 10.1029/2009GL041067.

Vicente-Serrano, Sergio M.; Beguería, Santiago; López-Moreno, Juan I. (2010): A Multiscalar Drought Index Sensitive to Global Warming. The Standardized Precipitation Evapotranspiration Index. In *J. Climate* 23 (7), pp. 1696–1718. DOI: 10.1175/2009JCLI2909.1.

Vicente-Serrano, Sergio M.; Beguería, Santiago; Lorenzo-Lacruz, Jorge; Camarero, Jesús Julio; López-Moreno, Juan I.; Azorin-Molina, Cesar et al. (2012a): Performance of Drought Indices

for Ecological, Agricultural, and Hydrological Applications. In *Earth Interact.* 16 (10), pp. 1–27. DOI: 10.1175/2012EI000434.1.

Vicente-Serrano, Sergio M.; Lopez-Moreno, Juan-I; Beguería, Santiago; Lorenzo-Lacruz, Jorge; Sanchez-Lorenzo, Arturo; García-Ruiz, José M. et al. (2014): Evidence of increasing drought severity caused by temperature rise in southern Europe. In *Environ. Res. Lett.* 9 (4), p. 44001. DOI: 10.1088/1748-9326/9/4/044001.

Vicente-Serrano, Sergio M.; López-Moreno, Juan I. (2005): Hydrological response to different time scales of climatological drought: an evaluation of the Standardized Precipitation Index in a mountainous Mediterranean basin. In *Hydrol. Earth Syst. Sci.* 9, pp. 523–533, checked on 12/9/2016.

Vicente-Serrano, Sergio M.; López-Moreno, Juan I.; Beguería, Santiago; Lorenzo-Lacruz, Jorge; Azorin-Molina, Cesar; Morán-Tejeda, Enrique (2012b): Accurate Computation of a Streamflow Drought Index. In *J. Hydrol. Eng.* 17 (2), pp. 318–332. DOI: 10.1061/(ASCE)HE.1943-5584.0000433.

WMO (2006): Drought monitoring and early warning: concepts, progress and future challenges. Weather and climate information for sustainable agricultural development. World Meteorological Organization, Geneva. Available online at http://www.droughtmanagement.info/literature/WMO_drought_monitoring_early_warning_2006.pdf, checked on 3/3/2017.

WMO (2012): Standardized Precipitation Index. User Guide. World Meteorological Organization, Geneva. Available online at http://www.wamis.org/agm/pubs/SPI/WMO_1090_EN.pdf, checked on 3/20/2017.

Yu, Jingjie; Fu, Guobin; Cai, Wenju; Cowan, Tim (2010): Impacts of precipitation and temperature changes on annual streamflow in the Murray–Darling Basin. In *Water International* 35 (3), pp. 313–323. DOI: 10.1080/02508060.2010.484907.

Zhang, Xiaoyong Sophie; Amirthanathan, Gnanathikkam E.; Bari, Mohammed A.; Laugesen, Richard M.; Shin, Daehyok; Kent, David M. et al. (2016): How streamflow has changed across Australia since the 1950s. Evidence from the network of hydrologic reference stations. In *Hydrol. Earth Syst. Sci.* 20 (9), pp. 3947–3965. DOI: 10.5194/hess-20-3947-2016.

8 ANNEX

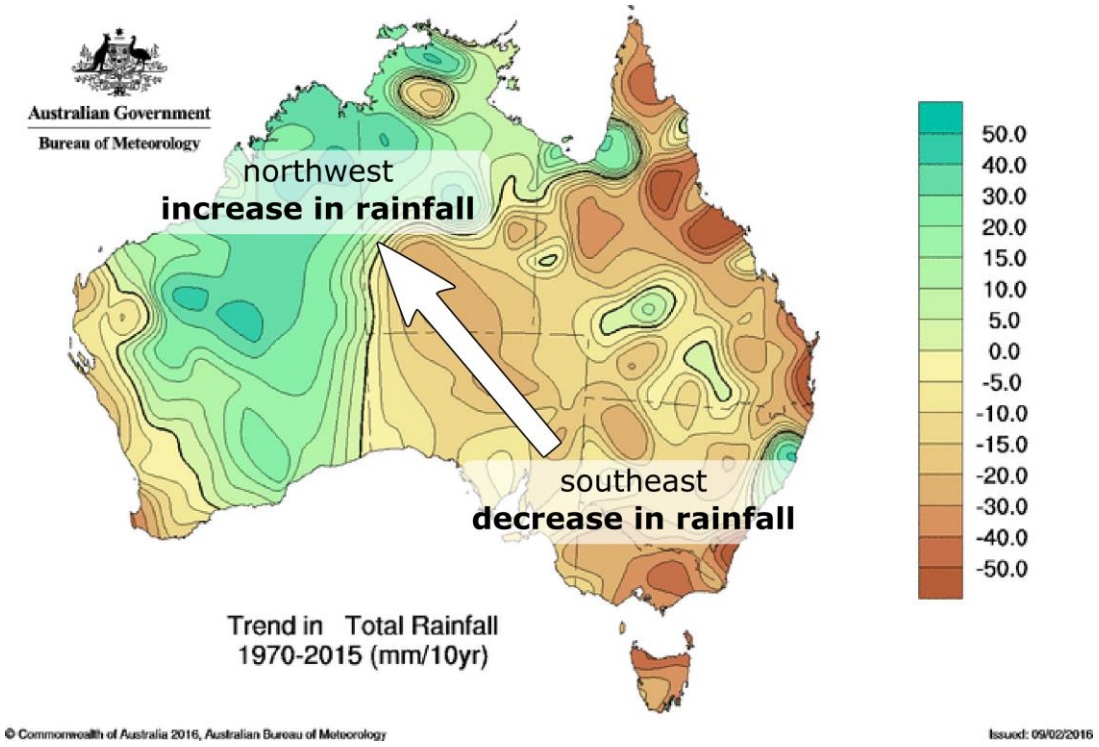

Annex 1: Annual rainfall trend in Australia (1970 - 2015). Modified from http://www.bom.gov.au/climate/change/#tabs=Tracker&tracker=trend-maps&tQ=map%3Drain%26area%3Daus%26season%3D0112%26p eriod%3D1970

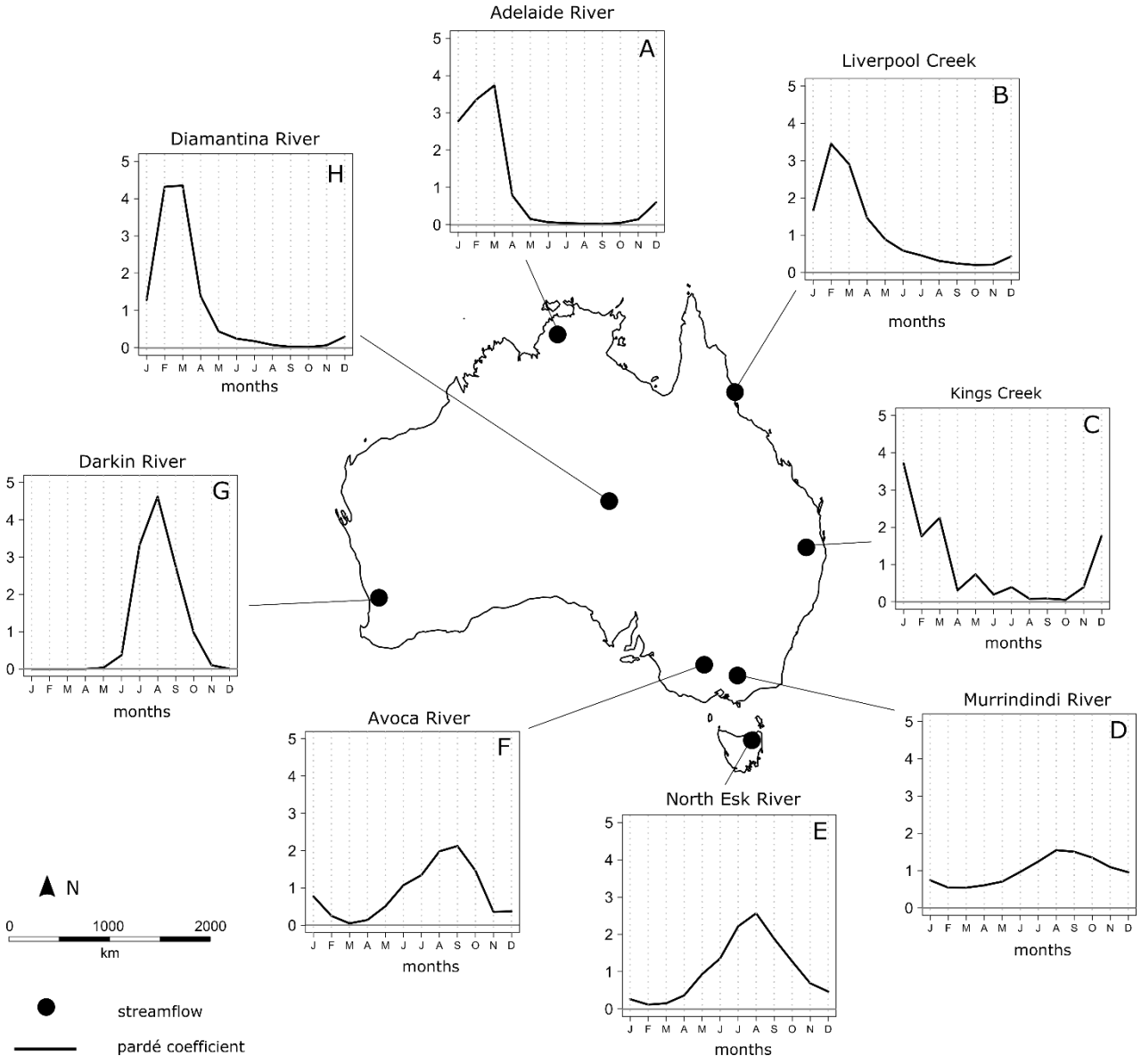

Annex 2: Pardé coefficients in Australia

Abbreviations

AUC	Area under the ROC curve
CSM	Computed Soil Moisture
ENSO	El Niño Southern Oscillation
GenEV	Generalized extreme value (distribution)
GenLOG	Generalized logistic (distribution)
GVAP	Gross Value Agricultural Production
IOD	Indian Ocean Dipole
MDRB	Murray-Darling River Basin
MJO	Madden-Julian oscillation
NSW	New South Wales (federal state)
PDSI	Palmer Drought Severity Index
PET	Potential evapotranspiration
QLD	Queensland (federal state)
ROC	Receiver Operating Characteristic
SA	South Australia (federal state)
SAM	Southern Annular Mode
SPEI	Standardized Precipitation and Evapotranspiration Index
SPI	Standardized Precipitation Index
SSI	Standardized Streamflow Index
VIC	Victoria (federal state)

Symbols

α	Parameter in logistic regression
β	Parameter in logistic regression
A	Quality code for runoff data (“best”)
B	Quality code for runoff data (“good”)
G	Quality code for runoff data (“gap-filled”)
$flow_{>10}$	Months at which the streamflow was higher than the 10^{th} percentile
$flow_{10}$	Months at which the streamflow was lower than the 10^{th} percentile
PET	Potential evapotranspiration
R_a	Mean monthly external radiation in Hargreaves formula (MJ / m^{-2} * $month^{-1}$)
T	Mean monthly temperature in Hargreaves formula ((Tmax + Tmin) / 2)
TR	Monthly temperature range in Hargreaves formula (Tmax - Tmin)

Ehrenwörtliche Erklärung

Hiermit versichere ich, die vorliegende Arbeit selbstständig verfasst zu haben. Ich habe keine anderen als die angegebenen Quellen und Hilfsmittel benutzt und alle wörtlich oder sinngemäß aus anderen Werken übernommenen Inhalte als solche kenntlich gemacht.

Die eingereichte Masterarbeit war oder ist weder vollständig noch in wesentlichen Teilen Gegenstand eines anderen Prüfungsverfahrens.

Die elektronische Version der eingereichten Masterarbeit stimmt in Inhalt und Formatierung mit den auf Papier ausgedruckten Exemplaren überein.

Christoph Ries

Freiburg im Breisgau, 9. Mai 2017